

Current Biology

Intrinsic maturation of sleep output neurons regulates sleep ontogeny in *Drosophila*

Highlights

- Juvenile flies spend more time in deep sleep compared with mature flies
- Elevated juvenile sleep drive is distinct from sleep rebound in mature flies
- Manipulating key sleep cells differentially affects juvenile and mature sleep
- Sleep output neurons exhibit distinct molecular signatures at different ages

Authors

Naihua N. Gong,
Hang Ngoc Bao Luong, An H. Dang, ...,
Karl Schmeckpeper, Roberto Bonasio,
Matthew S. Kayser

Correspondence

kayser@penmedicine.upenn.edu

In brief

All animals, from humans to flies, sleep more when young. The molecular determinants of sleep during early life remain largely unknown. Using non-invasive probabilistic approaches, Gong et al. define the changes in sleep architecture that occur with maturation in *Drosophila*. Their findings provide a novel insight into the mechanisms of sleep ontogeny.



Article

Intrinsic maturation of sleep output neurons regulates sleep ontogeny in *Drosophila*

Naihua N. Gong,^{1,2} Hang Ngoc Bao Luong,¹ An H. Dang,¹ Benjamin Mainwaring,¹ Emily Shields,^{3,4} Karl Schmeckpeper,⁵ Roberto Bonasio,⁴ and Matthew S. Kayser^{1,2,6,7,8,*}

¹Department of Psychiatry, Perelman School of Medicine at the University of Pennsylvania, Philadelphia, PA 19104, USA

²Department of Neuroscience, Perelman School of Medicine at the University of Pennsylvania, Philadelphia, PA 19104, USA

³Department of Urology and Institute of Neuropathology, Medical Center-University of Freiburg, 79106 Freiburg, Germany

⁴Epigenetics Institute and Department of Cell and Developmental Biology, Perelman School of Medicine at the University of Pennsylvania, Philadelphia, PA 19104, USA

⁵Department of Computer Science, University of Pennsylvania, Philadelphia, PA 19104, USA

⁶Chronobiology and Sleep Institute, Perelman School of Medicine at the University of Pennsylvania, Philadelphia, PA 19104, USA

⁷Twitter: @kayserlab

⁸Lead contact

*Correspondence: kayser@pennmedicine.upenn.edu

<https://doi.org/10.1016/j.cub.2022.07.054>

SUMMARY

The maturation of sleep behavior across a lifespan (sleep ontogeny) is an evolutionarily conserved phenomenon. Mammalian studies have shown that in addition to increased sleep duration, early life sleep exhibits stark differences compared with mature sleep with regard to sleep states. How the intrinsic maturation of sleep output circuits contributes to sleep ontogeny is poorly understood. The fruit fly *Drosophila melanogaster* exhibits multifaceted changes to sleep from juvenile to mature adulthood. Here, we use a non-invasive probabilistic approach to investigate the changes in sleep architecture in juvenile and mature flies. Increased sleep in juvenile flies is driven primarily by a decreased probability of transitioning to wake and characterized by more time in deeper sleep states. Functional manipulations of sleep-promoting neurons in the dorsal fan-shaped body (dFB) suggest that these neurons differentially regulate sleep in juvenile and mature flies. Transcriptomic analysis of dFB neurons at different ages and a subsequent RNAi screen implicate the genes involved in dFB sleep circuit maturation. These results reveal that the dynamic transcriptional states of sleep output neurons contribute to the changes in sleep across the lifespan.

INTRODUCTION

Across species, sleep duration peaks in early life and declines with age.^{1–5} Early life sleep is also characterized by differences in sleep architecture compared with maturity. For example, in humans, sleep duration as well as percentage of time spent in rapid eye movement (REM) sleep is highest in newborn infants and decreases with age.⁴ Several lines of evidence point toward the importance of early life sleep for normal neurodevelopment.^{2,6–11} Juvenile sleep may thus have characteristics that fulfill specific needs for nervous system development. However, mechanisms underlying sleep ontogeny—the change in sleep features across development—are largely unknown.

The probability of transitioning between sleep and wake influence sleep duration. These transitions are controlled by an interplay between sleep-regulatory neural substrates.^{12–14} In addition, both mammals and invertebrates such as *Drosophila melanogaster* exhibit transitions between distinct sleep stages, which are defined by electrophysiologic and behavioral measurements.^{15–22} In *Drosophila*, conditional probabilities of activity/inactivity state transitions as well as hidden Markov modeling (HMM) of sleep/wake substates have proven to be useful, non-invasive methods for probing the neurobiology underlying sleep

architecture.²³ Using such approaches toward a detailed analysis of sleep/wake transitions and sleep states in juvenile flies has yet to be explored.

How does the development of sleep-regulatory circuits influence changes to sleep architecture across the lifespan? In flies, maturation of a key sleep circuit in the central complex of the brain contributes to sleep ontogenetic changes. Specifically, juvenile flies exhibit increased activity in sleep-promoting neurons of the dorsal fan-shaped body (dFB) compared with mature flies.² One factor governing this change in sleep output is the maturation of dopaminergic (DA) inputs that inhibit dFB activity.^{24–26} These DA inputs are both less numerous and less active in juvenile flies, leading to increased dFB activity compared with mature flies.^{2,27} However, whether sleep-promoting dFB neurons themselves also undergo intrinsic maturation is unknown.

Using a conditional probabilities approach applied to locomotor measurements and HMM of sleep/wake substates,²³ we address the question of how sleep architecture differs between juvenile and mature *Drosophila*. We find excess sleep in juvenile flies is driven primarily by a decreased probability of flies transitioning out of sleep. Juvenile flies additionally spend proportionally more time in a deep sleep state compared with mature flies. In mature flies, activation of sleep-promoting neurons defined by



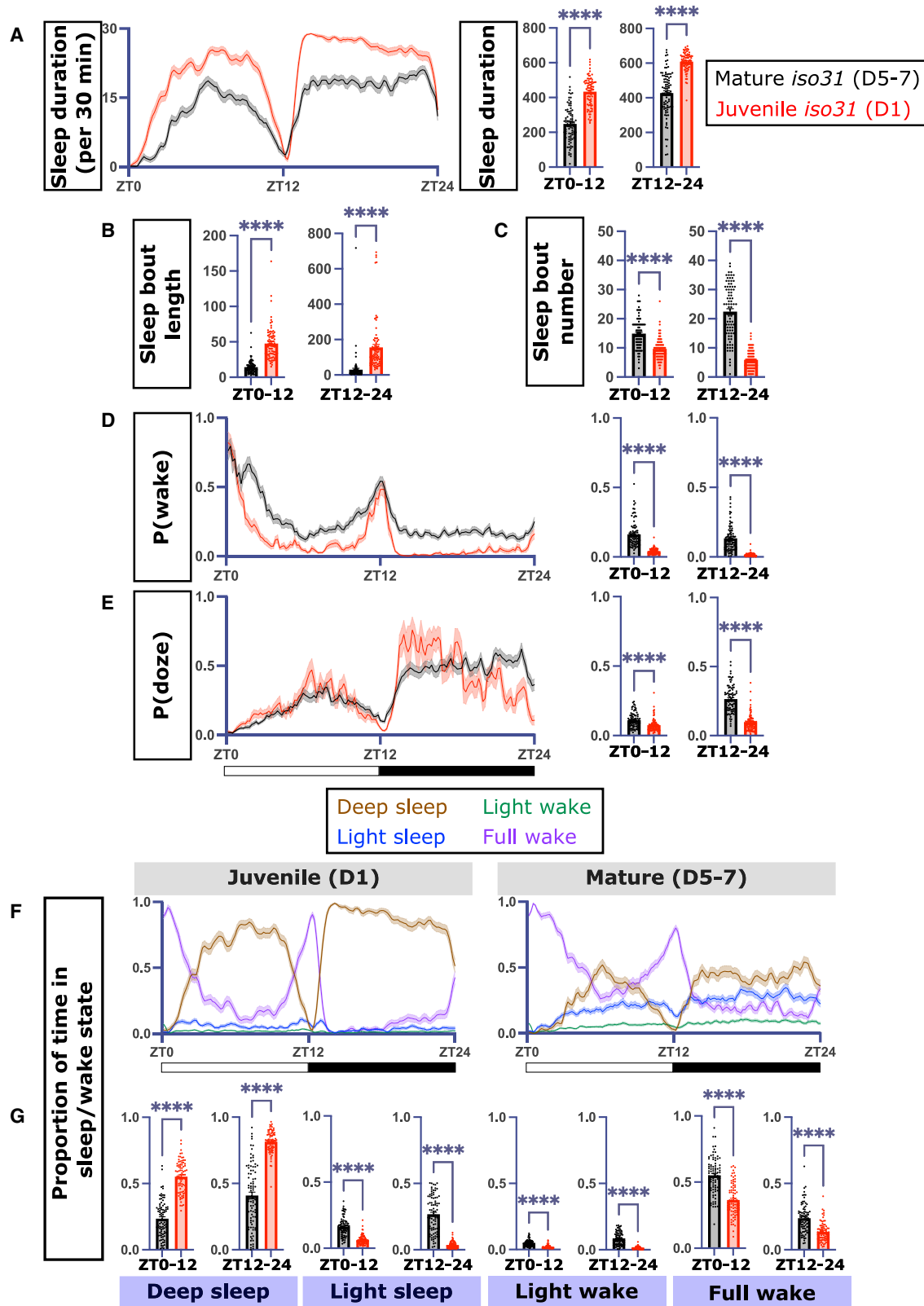


Figure 1. Excess deep sleep in juvenile flies results from decreased probability of transitioning from sleep to wake

(A–E) Sleep duration (A), average bout length (B), average bout number (C), P(wake) (D), and P(doze) (E) in mature (black, n = 87) versus juvenile (red, n = 82) *iso31* flies. Left: sleep metric traces. Right: quantification of sleep metrics across the lights-on (ZT0–12) or lights-off (ZT12–24) periods.

(legend continued on next page)

R23E10-GAL4 increases sleep duration but yields sleep architecture distinct from the juvenile sleep state. Conversely, inhibition of the same dFB neurons in juvenile flies does not result in mature fly sleep architecture. Finally, we find the dFB exhibits distinct molecular signatures throughout the period of sleep maturation, supporting the idea of an evolving role for the dFB across development. An RNAi-based screen of differentially expressed genes (DEGs) identifies *ringer* as involved in the anatomical and functional maturation of dFB sleep neurons. Our results indicate that intrinsic maturation of sleep output neurons contributes to sleep ontogenetic changes.

RESULTS

Juvenile flies exhibit increased deep sleep compared with mature flies

To investigate how sleep/wake transition probabilities differ between juvenile (1 day post-eclosion) and mature (5–7 days post-eclosion) adult flies, we recorded sleep in unmated *iso31* female flies using a high-resolution multibeam *Drosophila* activity monitoring (DAM) system. Consistent with previous studies,^{2,3,28} we observed greater total sleep duration, increased average sleep bout length, and decreased sleep bout number both during the day (ZT0–12) and night (ZT12–24) in juvenile flies compared with mature flies (Figures 1A–1C and S1A). These metrics are consistent with more consolidated sleep in juvenile compared with mature flies.^{2,27} P(wake) is defined as the probability of transitioning from an inactive to an active state, whereas P(doze) is the probability of transitioning from an active to inactive state.²³ P(wake) was significantly decreased during the day and the night in juvenile flies (Figures 1D and S1B), suggesting that increased sleep duration in juvenile flies is driven by a lower probability of transitioning from sleep to wake. Overall, P(doze) was also decreased in juvenile flies during the day and night (Figure 1E); however, this measure exhibited far more temporal variability, with specific periods in which juvenile flies exhibited increased P(doze) (for example, ZT3–6 and ZT15–18; Figure S1C). Previous work has established that P(doze) is less closely correlated with sleep duration than P(wake),²³ consistent with our observation that P(wake) is consistently decreased in juvenile flies and drives increased sleep duration. We also noted more variance in P(doze) in juvenile flies compared with mature when measured during 30-min windows (Figures S1D and S1E), likely because young flies spend so much time asleep that transitioning from wake to sleep is a relatively rare event over this short period of time.

Next, we asked how sleep/wake stages differ between juvenile and mature flies. In the presence of an arousing stimulus during sleep, juvenile flies are less likely to wake compared with their mature counterparts.² In *Drosophila*, an increased arousal threshold is indicative of a deeper sleep state,²³ but the proportion of time spent in specific sleep states across the lifespan is unknown. Locomotor recording followed by HMM has been

successfully used as a non-invasive method to establish physiologically relevant sleep/wake substates from DAM system activity measurements.²³ We trained two HMMs with four hidden substates (deep sleep, light sleep, light wake, and full wake) using activity measurements²³ from mature or juvenile *iso31* flies (Tables S1A and S1B; STAR Methods section for extended information regarding terms of constraints in the trained model). This same approach has previously been used to demonstrate progressively increased arousal thresholds with deeper sleep states in mature flies.²³ To determine whether transition and emission probabilities of the HMMs trained on mature and juvenile datasets (HMM-mature and HMM-juvenile) differed, we calculated the probability that HMM-mature or HMM-juvenile exactly fit observed activity patterns of each fly. For both juvenile and mature fly datasets, HMM-mature and HMM-juvenile yielded slightly different probabilities (Figures S2A and S2B), suggesting the characteristics of defined sleep/wake substates are dynamic across the lifespan. Applying HMM-mature and HMM-juvenile to the datasets yielded minor differences in the proportion of time spent in each of the four substates for both mature and juvenile flies. Despite these distinctions, the trends in substate differences between mature and juvenile flies were the same, regardless of the model used (Figures S2C–S2F), showing either model can be applied to observe biologically relevant differences in sleep states between juvenile and mature flies. We applied the HMM trained on mature fly activity to determine the proportion of time juvenile and mature flies spent in each of the four substates (Figures 1F, 1G, and S1F). Compared with mature flies, juvenile flies spent significantly more time in deep sleep across both the day and night. This proportional increase came at the expense of light sleep, light wake, and full wake (Figure 1G). Additional analysis of flies at post-eclosion day 3 demonstrated that changes to sleep duration, P(wake), and sleep substates are progressive across the first week of adulthood (Figure S3). The propensity for juvenile flies to spend more time in a less-arousable deep sleep state may therefore explain the lower probability of transitioning from sleep to wake. Finally, we examined whether ontogenetic changes in sleep substates are correlated with sleep duration. We found in both juvenile and mature flies that deep sleep was positively correlated with sleep duration, whereas full wake was negatively correlated (Figure S4). Thus, sleep duration is a strong driver of sleep substate, regardless of age.

To determine whether developmental changes in sleep/wake substates are consistent across different genetic backgrounds, we examined *Canton-S* (CS) and *w¹¹¹⁸* strains. Juvenile flies exhibited increased total sleep duration and sleep bout length (Figures 2A and 2B); sleep bout number was decreased at night in CS and *w¹¹¹⁸* juvenile flies and increased during the day in CS juvenile flies (Figure 2B). Although the difference between juvenile and mature fly sleep duration and bout characteristics was less pronounced in *w¹¹¹⁸*, similar trends were present. Consistent with our observations in *iso31* flies, P(wake) was decreased

(F) Deep sleep (brown), light sleep (blue), light wake (green), and full wake (purple) traces in juvenile (left) and mature (right) *iso31* flies.

(G) Quantification of proportion of time spent in each sleep stage across the lights-on or lights-off periods (Mann-Whitney U tests for all graphs in this figure). For this and all subsequent figures, sleep metric traces are generated from a rolling 30-min window sampled every 10 min unless otherwise specified.

For all graphs in this figure and other figures, data are presented as mean ± SEM. Significance values within figures are denoted as follows: *p < 0.05, **p < 0.01, ***p < 0.001, ****p < 0.0001. See also Figures S1–S5 and Table S1.

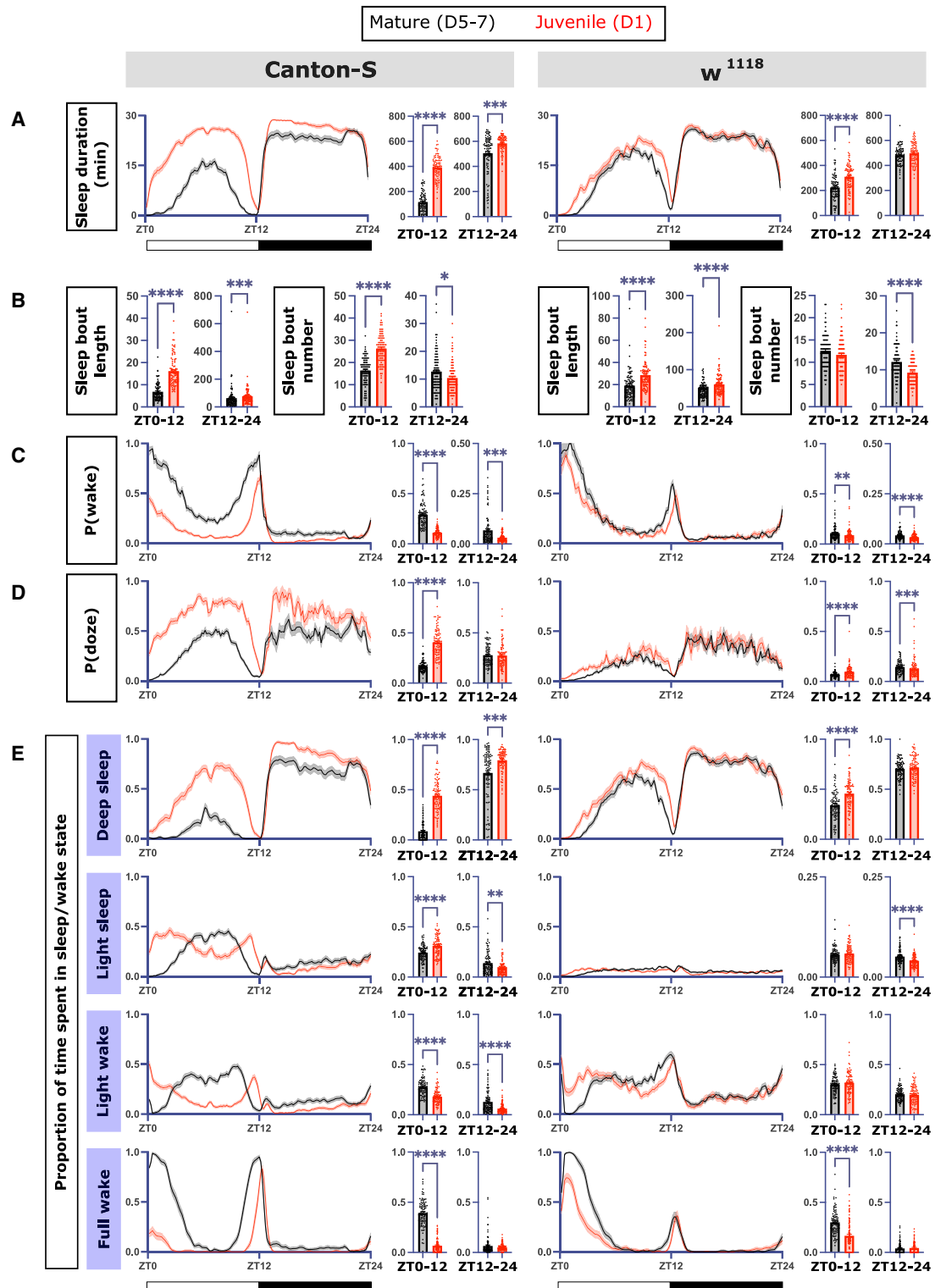
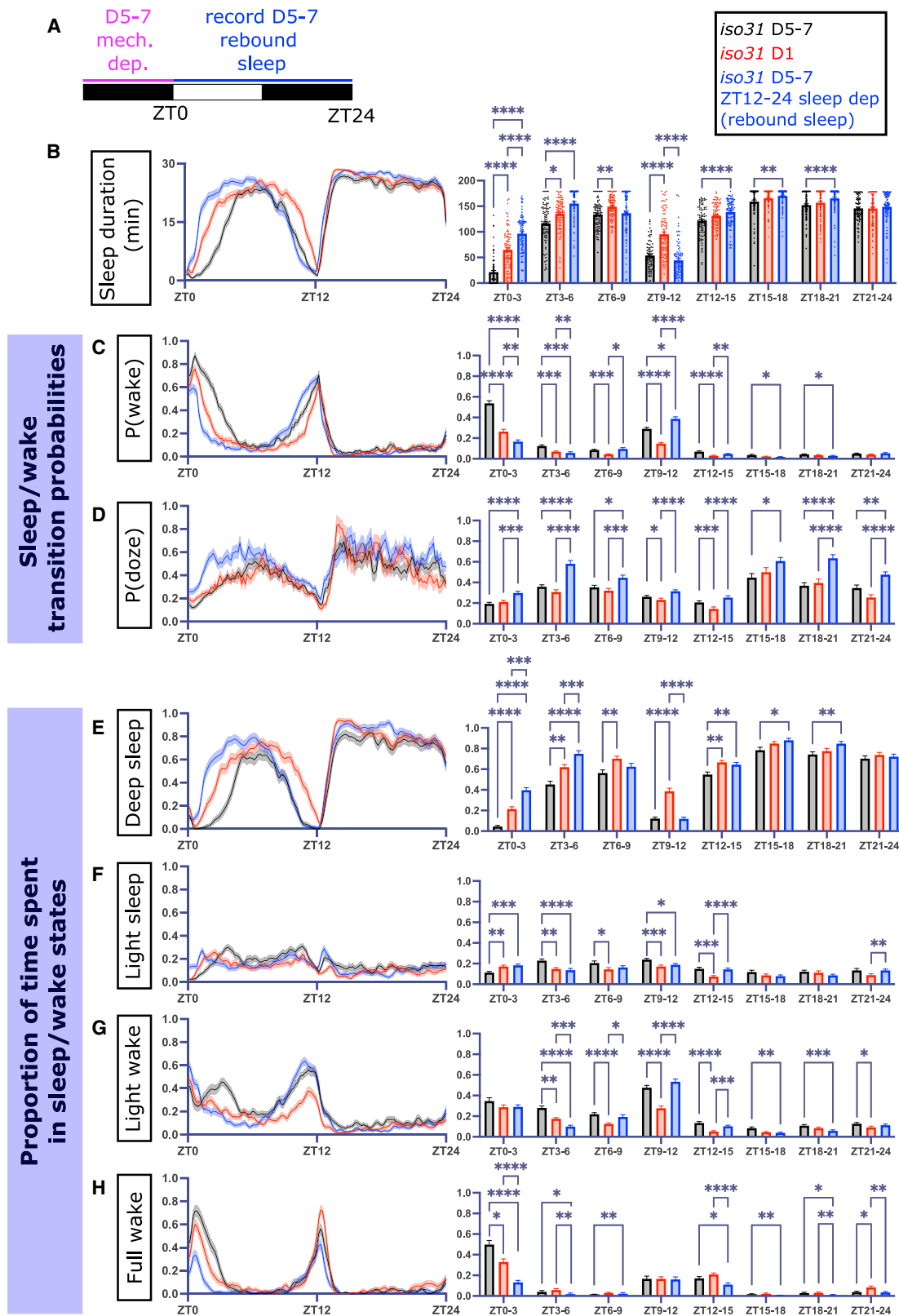


Figure 2. Ontogenetic changes in P(wake) and deep sleep are conserved across genetic backgrounds

(A–D) Sleep duration (A), average bout length and number (B), P(wake) (C), and P(doze) (D) in mature (black) versus juvenile (red) CS (left; $n = 95$ for mature and $n = 93$ for juvenile flies) and w^{1118} flies (right; $n = 96$ for mature and $n = 95$ for juvenile flies).

(E) Proportion of time spent in deep sleep, light sleep, light wake, and full wake in juvenile and mature CS (left) and w^{1118} flies (right). Left: sleep metric traces. Right: quantification of sleep metrics across the lights-on (ZT0–12) or lights-off (ZT12–24) periods (Mann-Whitney tests for all graphs in this figure).

For all graphs in this figure and other figures, data are presented as mean \pm SEM. Significance values within figures are denoted as follows: * $p < 0.05$, ** $p < 0.01$, *** $p < 0.001$, **** $p < 0.0001$. See also Table S1.



(legend on next page)

in juvenile flies (Figure 2C). P(doze) exhibited more variable differences across strains: although both CS and w^{1118} juvenile flies exhibited increased P(doze) during the day, there was no significant difference compared with mature CS flies at night, and P(doze) was decreased at night compared with mature w^{1118} flies (Figure 2D). These findings reflect the variable nature of P(doze), underscoring that developmental changes in P(doze) may not represent consistent ontogenetic effects. We then trained two separate HMMs based on activity patterns of mature CS or w^{1118} flies (Tables S1C and S1D) in order to assess sleep/wake states changes. Juvenile CS and w^{1118} flies exhibited increased deep sleep and decreased full wake (Figure 2E) compared with their mature counterparts, particularly from ZT0–12. In contrast to *iso31* flies, light sleep and light wake were variably different across age groups in CS and w^{1118} flies (Figure 2E). Together, our data show consistent developmental differences in P(wake), deep sleep, and full wake, regardless of genetic background, indicating that these are conserved ontogenetic aspects of sleep architecture.

Mated female flies sleep less and exhibit increased sleep fragmentation compared with their unmated counterparts.^{29,30} In our initial experiments, mature flies were unmated to control for this variable in comparison with juvenile flies, which are too young at time of collection to have mated. We next compared mature mated and unmated *iso31* female flies to address potential differences based on mating status. Mated mature flies exhibited decreased total sleep duration (Figure S5A) and bout duration (Figure S5B) across both the day and the night; sleep bout number was decreased during the day but increased at night (Figure S5C), consistent with increased nighttime sleep fragmentation. P(wake) was consistently increased during both the day and night in mated flies (Figure S5D), whereas P(doze) was decreased during the day and increased at night in mated flies (Figure S5E). Mated flies spent less time in deep sleep during both the day and the night, which was redistributed to time in full wake during the day and night and increased light sleep and light wake time at night (Figure S5F). These results suggest that mating not only decreases sleep duration as previously described but also additionally affects the sleep architecture of female flies: mated flies are more likely to wake from sleep and spend more time in light sleep and wake states at the expense of deep sleep, especially during the day. To control for the effect of mating on sleep, we compared unmated mature flies with juvenile flies in subsequent experiments.

The juvenile sleep state is distinct from rebound sleep in deprived mature flies

Following sleep deprivation, rebound sleep in mature flies is characterized by increased sleep duration as well as increased P(doze).²³ Does sleep architecture in juvenile flies appear similar

to a sleep-deprived mature fly? To test this directly, we mechanically sleep deprived mature *iso31* flies from ZT12–24 and recorded rebound sleep in single beam activity monitors (necessitated by the method of deprivation) during the entire 24-h period afterward (Figure 3A). We first binned our analyses into 12-h intervals (Figures S6A–S6F) and noted less pronounced nighttime differences in sleep duration between juvenile and mature flies, presumably due to lower spatial resolution of the activity monitors. Nonetheless, deprived mature flies slept significantly more than non-deprived mature controls both during the day and night, with comparable total sleep duration compared with juvenile flies (Figure S6A). Sleep bout length was significantly increased in rebounding mature flies during the day (Figure S6B), whereas bout number remained unchanged in rebounding mature flies (Figure S6C). P(wake) was decreased in rebounding mature flies during the day but was unchanged at night compared with non-deprived controls (Figure S6D). Strikingly, P(doze) following deprivation was increased both during the day and night compared with either juvenile or mature control flies (Figure S6E). These results emphasize the utility of sleep/wake transition probabilities to understand unique aspects of sleep fragmentation beyond sleep bout length and number: although rebounding mature flies exhibit similar bout characteristics as juvenile flies (Figures S6B and S6C), there are marked differences in P(doze) that are not reflected solely by bout length or number (Figure S6E). Finally, regarding sleep/wake states, deep sleep was significantly increased in rebounding mature flies compared with mature controls during both the day and night, whereas full wake was significantly decreased even in comparison with juvenile controls (Figure S6F).

Next, we binned the data into 3-h intervals to assess sleep architecture changes with greater temporal resolution. During the day, deprived mature flies slept significantly more than control mature flies and juvenile flies from ZT0–6, after which sleep duration tapered off to non-deprived mature fly levels (Figure 3B). At night, deprived flies continued to exhibit increased sleep compared with non-deprived controls from ZT12–21 (Figure 3B). P(wake) in rebounding mature flies was decreased compared with control mature flies from ZT0–6 and ZT15–21 (Figure 3C), whereas P(doze) was increased during ZT0–9 and ZT15–24 compared with mature controls. Of note, although sleep duration in deprived mature flies and juvenile flies was comparable from ZT6–9 and throughout ZT12–24 (Figure 3B), P(doze) in deprived mature flies remained elevated across the entire day and night periods compared with juvenile flies (Figures 3D and S6E). Finally, we assessed sleep substates (Figures 3E–3H) and found that deep sleep was significantly increased in rebounding mature flies, although the deep sleep changes did not persist across the entire day as in juvenile flies (Figure 3E); however, rebounding mature flies continued to exhibit increases in deep

Figure 3. The juvenile sleep state is distinct from homeostatic sleep rebound in mature flies

(A) Schematic of deprivation period and period of recorded rebound sleep in mature flies.

(B–H) Sleep duration (B), P(wake) (C), P(doze) (D), and proportion of time spent in deep sleep (E), light sleep (F), light wake (G), and full wake (H) in non-deprived *iso31* mature flies (black, n = 85), juvenile *iso31* flies (red, n = 90), and rebounding mature *iso31* flies (blue, n = 90) (Kruskal-Wallis test with post hoc Dunn's multiple comparison test). Data shown are from ZT0–24 after previous overnight ZT12–24 deprivation. Left: sleep metric traces. Right: quantification of sleep metrics binned into 3-h windows across ZT0–24.

For all graphs in this figure and other figures, data are presented as mean ± SEM. Significance values within figures are denoted as follows: *p < 0.05, **p < 0.01, ***p < 0.001, ****p < 0.0001. See also Figure S6 and Table S1.

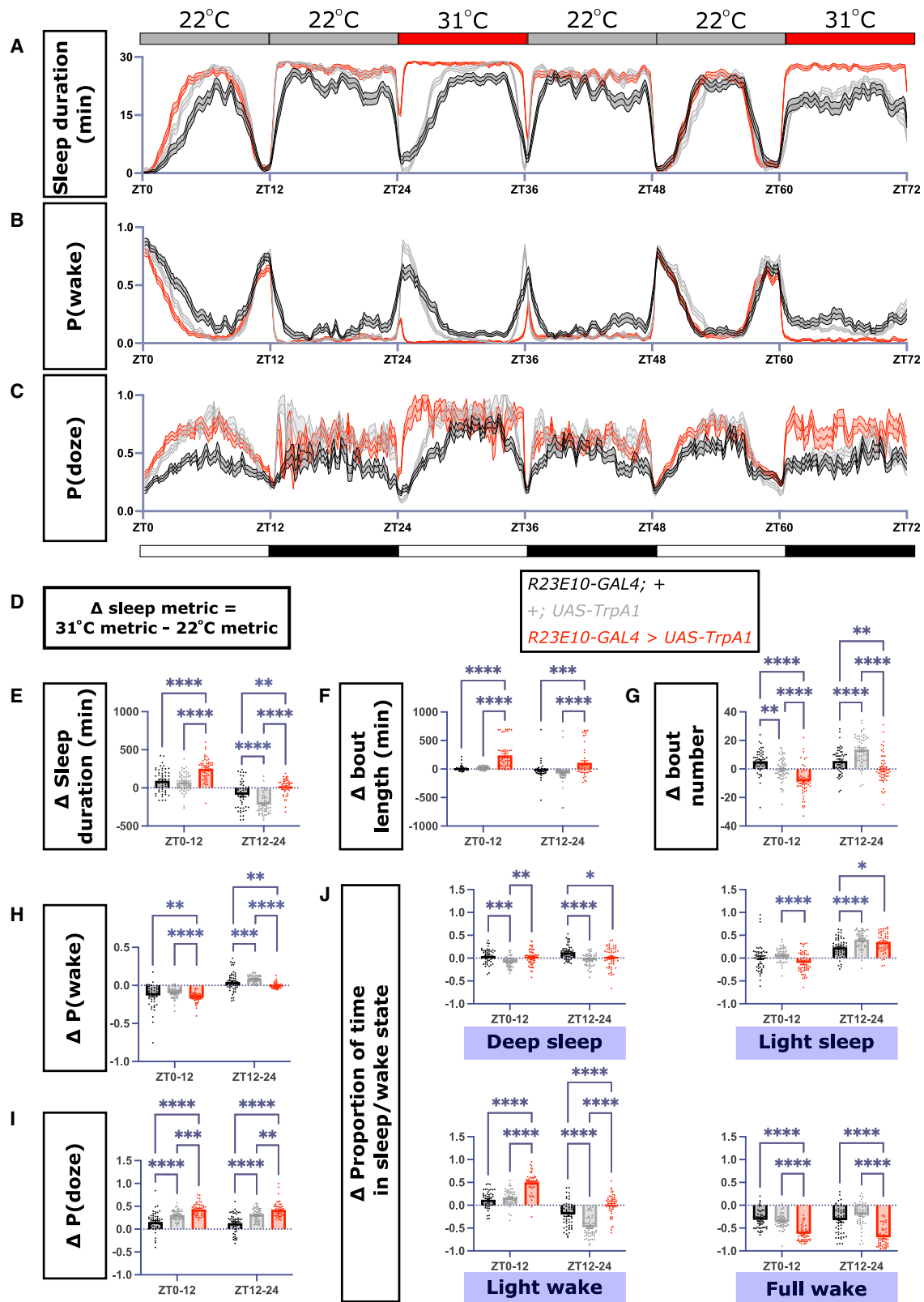


Figure 4. Activation of *R23E10-GAL4*+ neurons in mature flies does not fully recapitulate the juvenile sleep state

(A–C) Sleep duration (A), P(wake) (B), and P(doze) (C) sleep traces in *R23E10-GAL4 > UAS-TrpA1* (red, n = 53) flies and genetic controls (black, n = 51; gray, n = 53). Gray bars at the top denote periods at 22°C, whereas red bars denote periods at 31°C.

(legend continued on next page)

sleep into the night compared with control flies from ZT12–21 (Figure 3E). Together, these results support the idea that juvenile fly sleep is a unique state that is distinct from mature fly homeostatic sleep rebound.

Do juvenile flies respond to mechanical sleep deprivation in a similar manner compared with mature counterparts? Rebounding juvenile flies exhibited increased sleep duration during parts of both the day and night (Figure S6G), without major changes in sleep bout length or number (Figures S6H and S6I). Daytime P(wake) was decreased from ZT0–6 in sleep-deprived juvenile flies (Figure S6J), and P(doze) was increased during the day and night, both similar to mature flies (see Figure 3C). Rebounding juvenile flies additionally exhibited similarities to mature flies in sleep/wake substate changes (increased deep sleep and decreased full wake; Figure S6L). Together, these results show that changes in sleep architecture in the setting of homeostatic rebound sleep are conserved, regardless of age.

Sleep-promoting dorsal fan-shaped body neurons exhibit differential function between juvenile and mature flies

During sleep rebound following sleep deprivation, the dFB exhibits increased activity in mature flies.³¹ Since the dFB is also more active in juvenile flies,² we next asked whether activation of the dFB in mature flies results in a juvenile-like sleep state. We thermogenetically activated a sleep-promoting subset of dFB neurons using *R23E10-GAL4*^{31,32} to drive a heat-sensitive cation channel, *UAS-TrpA1*³³ (*R23E10-GAL4>UAS-TrpA1*) in mature flies. Compared with a baseline 24 h at 22°C (Figure 4D), raising the temperature to 31°C significantly increased sleep duration (Figures 4A and 4E) and bout length (Figure 4F) and decreased bout number (Figure 4G) during the day and the night compared with genetic controls in mature flies (Figures 4A and 4E). Activation of dFB neurons decreased P(wake) and increased P(doze) during both the day and the night (Figures 4B, 4C, 4H, and 4I). Activation of dFB neurons also increased light wake while decreasing full wake (Figure 4J). Time spent in light and deep sleep was not affected (Figure 4J). Thus, dFB neuron activation increases sleep in mature flies and mirrors some aspects of juvenile sleep, specifically differences in sleep bout length, sleep bout number, and P(wake); however, this manipulation fails to increase deep sleep, distinct from differences observed in juvenile flies, and also increases P(doze). These results underscore the utility of sleep/wake transition probabilities and HMM sleep substates in understanding sleep, revealing that dFB activation in mature flies does not fully recapitulate the juvenile sleep state.

Increased dFB activity is thought to drive increased sleep in juvenile flies,² leading us to ask the converse question of whether dFB inhibition in juvenile flies result in a mature-like sleep state. We drove expression of the inwardly rectifying potassium

channel, *Kir2.1*, in *R23E10-GAL4* neurons. To account for developmental effects of inhibiting the dFB, we utilized a ubiquitously expressed temperature-sensitive *GAL80* repressor protein (*tub-GAL80^{ts}*).³⁴ Raising the temperature rapidly degrades *GAL80^{ts}*, expressing the downstream *UAS* transgene. In juvenile flies, expressing *Kir2.1* in *R23E10-GAL4* neurons (*tub-GAL80^{ts}; R23E10-GAL4>UAS-Kir2.1*) decreased sleep duration during the night (Figures 5A–5C). Sleep/wake transition probabilities were unaffected with dFB inhibition in juvenile flies (Figures 5D and 5E); however, nighttime deep sleep was decreased, whereas light sleep and light wake increased (Figure 5F). Thus, dFB inhibition in juvenile flies did not fully reflect mature-like sleep architecture. Previous studies have shown that inhibition of the dFB in mature flies via ablation, transmitter knockdown, or chronic silencing can reduce sleep,^{24,25,31,32,35} but acute manipulations of dFB activity using sleep-neuron specific drivers have yielded mixed results.³⁶ How does inhibition of the dFB in mature flies affect sleep architecture? Driving *Kir2.1* expression in *R23E10-GAL4* neurons in mature did not reliably effect sleep duration (Figures 5G and 5H), sleep/wake transition probabilities (Figures 5I and 5J), or sleep/wake substates (Figure 5K) compared with parental controls. Consistent with previous work,³⁶ these results indicate that acute dFB inhibition in mature flies does not strongly affect daily sleep. Together, our findings suggest that the dFB regulates different aspects of sleep architecture in mature and juvenile flies.

Pdm3 knockdown abolishes developmental changes in P(wake) and deep sleep

How do molecular regulators of sleep ontogeny contribute to developmental changes in sleep states? *Pdm3* encodes a transcription factor that is necessary for patterning of DA arousal neurons involved in sleep maturation.²⁷ As previously described, knocking down *pdm3* in neurons using the *elav-GAL4* driver (*elav-GAL4>UAS-pdm3 RNAi*) abolished differences in sleep duration between juvenile and mature flies (Figure 6A). *Pdm3* knockdown caused sleep fragmentation in both age groups, but sleep bout length and number changes across development were largely unaffected (Figures 6B and 6C). We noted a redistribution in sleep duration from night to day in the setting of *pdm3* knockdown (Figure 6A), consistent with known circadian disruptions.²⁷ Thus, we assessed sleep/wake transition probabilities and time spent in sleep/wake substates across 24 h to control for independent circadian effects of *pdm3* knockdown. Although ontogenetic differences in P(wake) and deep sleep were intact in genetic controls, this effect was lost in the setting of *pdm3* knockdown (Figures 6D–6F). Interestingly, age-dependent differences in full wake remained intact, albeit diminished. Together, these results show *pdm3* knockdown interferes with normal maturation of sleep transitions and substates in addition to sleep duration.

(D) Formula used to calculate changes in sleep metrics. To account for differences in baseline sleep metrics at 22°C, changes in sleep metrics for individual flies was calculated.

(E–I) Changes in sleep duration (E), average sleep bout length (F), sleep bout number (G), P(wake) (H), and P(doze) (I) across ZT0–12 and ZT12–24.

(J) Changes in the proportion of time spent in deep sleep, light sleep, light wake, and full wake in the setting of thermogenetic *R23E10-GAL4* neuron activation (Kruskal-Wallis with post hoc Dunn's multiple comparison test).

For all graphs in this figure and other figures, data are presented as mean ± SEM. Significance values within figures are denoted as follows: *p < 0.05, **p < 0.01, ***p < 0.001, ****p < 0.0001. See also Table S1.

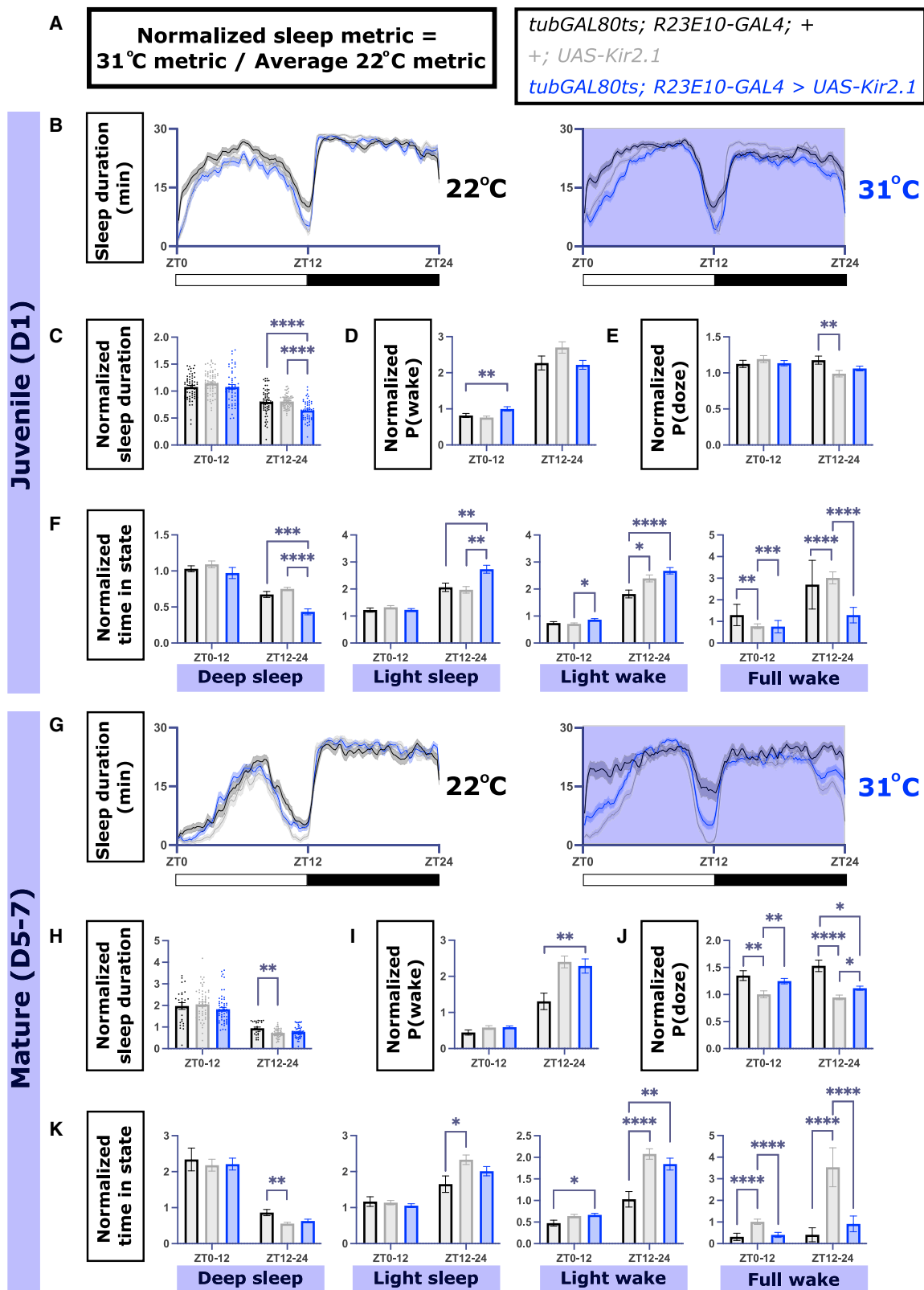


Figure 5. dFB inhibition decreases sleep duration in juvenile flies but does not recapitulate mature fly sleep architecture
 (A) Formula used to calculate normalized sleep metric. Sleep was recorded in juvenile flies 1 day post-eclosion, and sleep metrics were normalized to the average of the baseline at 22°C.

(legend continued on next page)

Distinct molecular profiles in juvenile versus mature dorsal fan-shaped body neurons reflect differential sleep-regulatory functions across lifespan

Maturation of DA projections to the dFB is a key event for sleep ontogeny,^{2,27} but whether sleep-promoting dFB neurons undergo intrinsic maturation is unknown. Single-cell RNA-seq analysis of the adult fly brain at different ages previously identified a cluster of cells that contain those matching the expression profile of *R23E10-GAL4* sleep-promoting neurons.³⁷ This cluster exhibited 55 DEGs between mature (day 9 post-eclosion) and juvenile (day 0–1 post-eclosion) flies (Figure 7A).³⁷ We used this dataset to ask how the transcriptomic profiles of dFB cells change during development. First, to identify mechanisms that might be responsible for dFB function in juvenile and mature flies, we performed gene set enrichment analysis (GSEA). GSEA^{38,39} revealed that DEGs more highly expressed in mature flies were enriched for ribosomal and translational processes (Table S2A). Conversely, although DEGs more highly expressed in juvenile flies were not significantly enriched for specific processes, we noted several of these genes were involved in transmembrane ion transport, synaptic transmission, and neurodevelopment (Table S2B). Thus, dFB cells exhibit distinct gene expression profiles in juvenile and mature flies.

Next, we sought to determine whether developmental changes in the molecular landscape of *R23E10-GAL4+* neurons relate to functional maturation of these cells. We reasoned that DEGs with higher expression in the juvenile compared with mature dFB cells could be involved in the post-eclosion development of this sleep center. Specifically, we hypothesized that knockdown of these genes would stunt dFB sleep neurons in a more juvenile state—thus, we would expect to observe juvenile-like sleep architecture in mature flies. Using the *R23E10-GAL4* driver, we individually knocked down 12 genes that were more highly expressed in the juvenile dFB neurons using 16 RNAi lines (Table S3) and recorded sleep using the multibeam DAM system in mature flies. When compared with genetic controls (*R23E10-GAL4>UAS-mCherry RNAi* and +; *UAS-DEG RNAi*), knockdown of DEGs with increased expression in juvenile flies did not differentially affect total sleep duration (Figure S7A), sleep bout length, or bout number (Figures S7C and S7D) during the day or night. However, focusing solely on sleep duration fails to capture more nuanced differences in sleep states between juvenile and mature flies. To examine sleep states, we trained an HMM on data from mature *R23E10-GAL4>UAS-mCherry RNAi* control flies to account for genetic background (Table S1G). We focused on P(wake), deep sleep, and full wake, as these metrics demonstrate robust ontogenetic changes. This approach did not identify any individual gene that, with knockdown, resulted in significant changes to all three of these sleep variables, or to P(doze), light sleep, or light wake (Figure S7). However, *R23E10-GAL4*-driven knockdown of *ringmaker* (*ringer*) was

associated with a decrease in full wake in mature flies compared with both genetic controls, without significant effects on other sleep measures (Figures 7B–7G and S7A–S7I). *Ringer* encodes a tubulin polymerization promoting protein (TPPP) involved in neurodevelopment,^{40,41} supporting the possibility that it may be important in dFB neuron maturation. Of note, knockdown of one of the RNAi lines for *14-3-3zeta* also decreased full wake in mature flies compared with genetic controls (Figure S7I; line 3, BL 41878). However, given the variable effects of knockdown across different RNAi lines, we chose to focus on *ringer*.

To further investigate how *ringer* knockdown might impact development of dFB neurons, we examined the morphology of *R23E10-GAL4* dFB projections in mature flies in the setting of *ringer* knockdown by driving the expression of *mCD8::GFP* in conjunction with *ringer* RNAi (*R23E10-GAL4>UAS-mCD8::GFP; UAS-ringer RNAi*). Knockdown of *ringer* decreased dFB volume compared with control flies (Figures 7H and 7J), reflecting reduced *R23E10-GAL4* neurite abundance in the dFB. Next, given that dFB neurons are normally more active in juvenile compared with mature flies,² we asked whether dFB activity in mature flies was altered by *ringer* knockdown. To measure this, we drove expression of a calcium-dependent GFP reporter (*CaLexA*, calcium-dependent nuclear import of LexA system)^{2,42} in the setting of *ringer* knockdown. Indeed, *ringer* knockdown was associated with an aberrant increase in activity in dFB neurons of mature flies compared with RNAi control (Figures 7I and 7K), suggesting *ringer* knockdown may affect the functional maturation of these cells. These results provide evidence that distinct biological processes present in juvenile fly dFB cells are important for *R23E10-GAL4* neuron maturation.

DISCUSSION

Sleep duration in early life is elevated across species, but how maturation of individual neural circuits contributes to ontogenetic changes in sleep architecture is unclear. In this study, we describe sleep/wake transition probabilities and substates in *Drosophila* that accompany changes in sleep duration across the lifespan. Using these probabilistic methods, we identify mechanisms underlying intrinsic dFB development that contribute to sleep maturation. Our results link changes in the molecular profile of sleep output neurons to sleep ontogeny.

Here, we demonstrate quantifiable differences in sleep architecture across the lifespan that extend beyond traditional measurements of sleep fragmentation, which utilize sleep bout length and number. How does the unique sleep quality in juvenile flies contribute to neurodevelopment? In developing mammals, REM and non-REM sleep are thought to play different roles.⁴³ The proportion of REM sleep is significantly increased in neonates⁴ and plays a critical role in plasticity of the developing visual cortex^{11,44,45} as well as selective strengthening of synaptic

(B and G) Sleep duration traces of juvenile (B) and mature (G) *tubGAL80ts; R23E10-GAL4>UAS-Kir2.1* (blue) versus genetic controls (black and gray) at 22°C (left) and 31°C (right).

(C–F and H–K) Normalized sleep duration (C), P(wake) (D), P(doze) (E), and time spent in each sleep state (F) in juvenile flies and mature flies (H–K, respectively). For juvenile flies, n = 75, 60, and 54 from left to right. For mature flies, n = 28, 56, and 58 from left to right (Kruskal-Wallis with post hoc Dunn's multiple comparison test).

For all graphs in this figure and other figures, data are presented as mean ± SEM. Significance values within figures are denoted as follows: *p < 0.05, **p < 0.01, ***p < 0.001, ****p < 0.0001. See also Table S1.

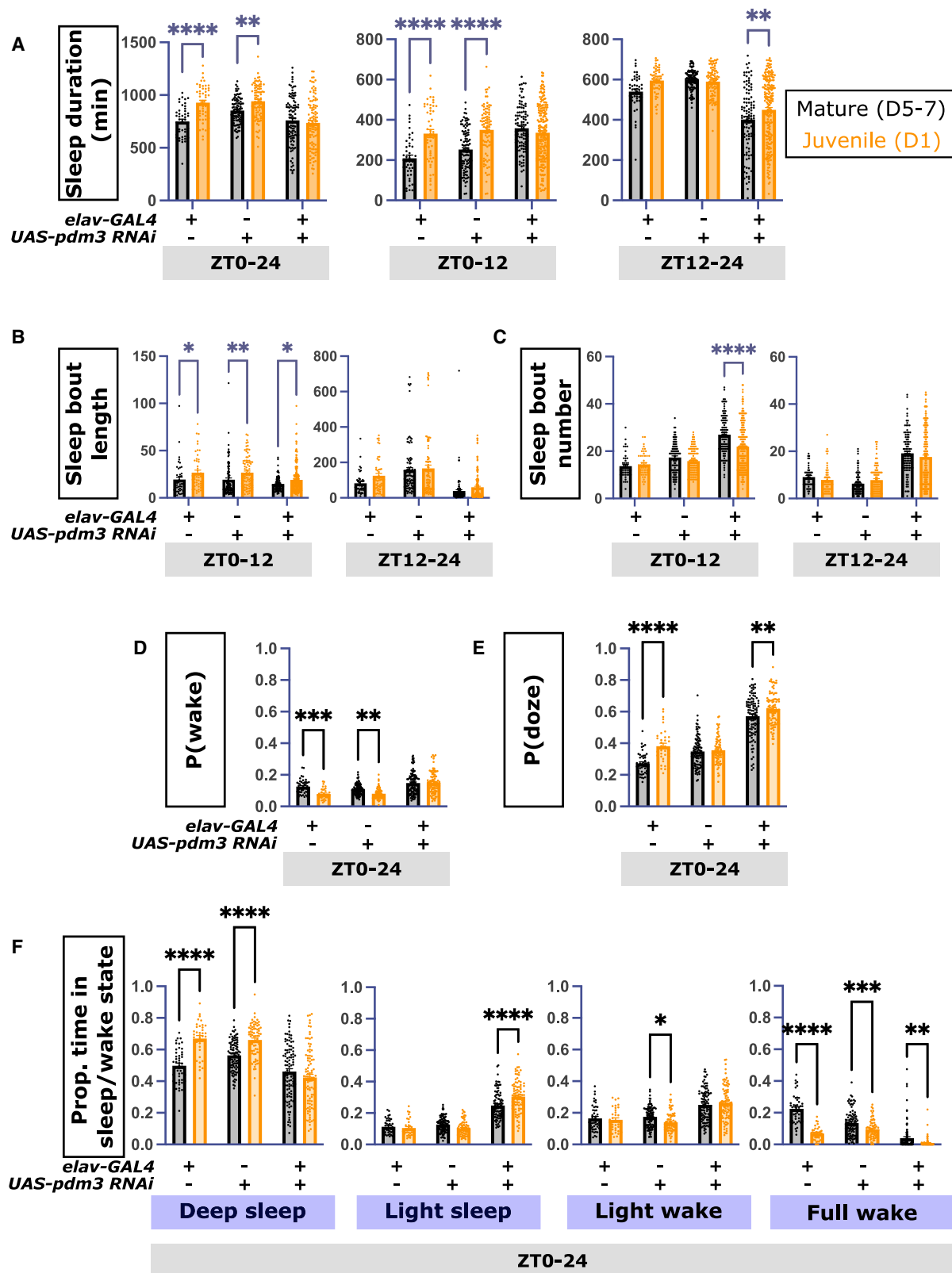


Figure 6. Ontogenetic changes in sleep architecture are lost in the setting of *Pdm3* knockdown

(A) Sleep duration in mature (black) and juvenile (orange) in genetic controls and *elav-GAL4>UAS-pdm3 RNAi* flies (left to right) during ZT0-24, ZT0-12, and ZT12-24.

(legend continued on next page)

contacts.⁴⁶ A preponderance of motor twitches also occurs during REM sleep in young animals, and increased REM is thought to be important for patterning of sensorimotor circuits.^{47–49} Despite these lines of evidence, we understand little about the genetic mechanisms linking REM sleep to brain development. Furthermore, non-REM sleep is proportionally decreased compared with REM sleep but still plays a role in synaptic pruning⁵⁰ and cortical maturation,⁵¹ especially during later developmental periods beyond the neonatal stage. However, as with REM sleep, the molecular mechanisms connecting non-REM sleep to neurodevelopment remain unknown. Our study establishes a genetically tractable model to identify molecular regulators of sleep states that are important for sleep-dependent neurodevelopment.

Development of arousal-promoting DA neurons is known to be important for normal sleep ontogeny.²⁷ *Pdm3* is a key factor in this process, and we show here that *pdm3* knockdown also disrupts the normal ontogenetic progression of sleep architecture. Beyond DA changes, we demonstrate that intrinsic maturation of sleep output neurons contributes to differences in sleep between mature and juvenile animals. The dFB normally exhibits increased activity in juvenile compared with mature flies, which results in excess sleep duration in early life.² Although dFB inhibition decreases daily sleep in juvenile flies, this manipulation does not result in “mature-like” sleep architecture. Conversely, although dFB activation in mature flies increases sleep duration, this sleep does not fully recapitulate the juvenile state. In mature flies, the dFB is involved in rebound following sleep deprivation, and disrupting the function of the dFB by knocking down various signaling components blunts rebound.^{31,32,35} These results suggest that the dFB regulates sleep during periods of increased homeostatic drive, such as during early life and in the sleep-deprived mature adult. However, several lines of evidence, including results presented here, demonstrate sleep in juvenile flies is distinct from rebound sleep in mature flies.³ Additionally, single-cell RNA-seq analysis reveals distinct molecular profiles in the dFB in juvenile flies compared with mature flies, supporting the hypothesis that these neurons undergo intrinsic development that may govern differential sleep-regulatory functions. Indeed, our functional studies suggest the sleep-promoting dFB neurons have a changing role in sleep across development: although they influence baseline sleep in juvenile flies, they play a more specific role in rebound sleep in mature flies.

Are the distinct molecular signatures present in juvenile fly dFB cells relevant for dFB development? Our results suggest *ringer*, a member of the TPPP family, may be important for dFB maturation: *ringer* knockdown decreases time spent in full wake in mature flies from ZT12–24. We suspect *ringer* is one of many molecules potentially involved in dFB maturation, and our work sets the stage for this future investigation. A limitation of the current study is that our findings cannot account

for how *ringer* knockdown specifically affects time spent in full wake, but not other sleep metrics. *Ringer* knockdown does impinge on the morphologic and functional maturation of dFB neurons. Additional work is needed to determine how such changes translate into alterations in sleep ontogeny, which would more precisely establish a role for *ringer* in *R23E10-GAL4* neuron maturation. However, in both vertebrates and invertebrates, TPPPs have been implicated both in neurodegeneration^{52,53} and neurodevelopment.^{40,54} *Ringer* is the only known *Drosophila* ortholog of mammalian TPPP.⁴⁰ Like other members of the TPPP family, *ringer* is involved in microtubule polymerization and stabilization important for neurite extension.^{40,41} One possibility is that *R23E10-GAL4* neurite elaboration in the dFB throughout the juvenile period is critical for appropriate connectivity with arousal-promoting DA inputs and eventual suppression of high sleep drive in the mature fly. Consistent with this idea, *ringer* knockdown leads to a reduction in *R23E10-GAL4* projection volume in the dFB in mature flies (Figure 7F). Another possibility lies in the heterogeneity of dFB sleep neurons: individual dFB neurons exhibit vastly different excitabilities,^{25,31} suggesting the dFB contains a diverse group of sleep cells. Knockdown of genes that are overexpressed in juvenile flies may inhibit the development of dFB neuronal subpopulations that are specifically relevant in mature flies. Intersectional approaches to investigate the contribution of specific subgroups of dFB neurons to sleep in juvenile and mature flies would be informative. Notably, knockdown of *ringer* did not affect total sleep duration or standard sleep bout characteristics, although we observed significant effects on time spent in full wake. These results highlight the utility of non-invasive computational approaches in the fly for investigating sleep and provide a framework for understanding molecular processes governing sleep ontogeny.

STAR★METHODS

Detailed methods are provided in the online version of this paper and include the following:

- KEY RESOURCES TABLE
- RESOURCE AVAILABILITY
 - Lead contact
 - Materials availability
 - Data and code availability
- EXPERIMENTAL MODEL AND SUBJECT DETAILS
- METHOD DETAILS
 - Sleep assays
 - Thermogenetic activation and inhibition experiments
 - Sleep/wake transition probabilities and hidden Markov modeling analysis
 - Single cell RNA-Seq analysis
 - Gene set enrichment analysis of differentially expressed dFB genes

(B and C) Average sleep bout length (B) and number (C) during ZT0–12 and ZT12–24.

(D–F) P(wake) (D), P(doze) (E), and proportion of time spent in deep sleep, light sleep, light wake, and full wake (F) in genetic controls compared with *elav-GAL4>UAS-pdm3 RNAi* flies. From left to right, n = 46, 35, 101, 76, 103, and 94 (two-way ANOVA with post hoc Sidak’s multiple comparison test).

For all graphs in this figure and other figures, data are presented as mean ± SEM. Significance values within figures are denoted as follows: *p < 0.05, **p < 0.01, ***p < 0.001, ****p < 0.0001. See also Table S1.

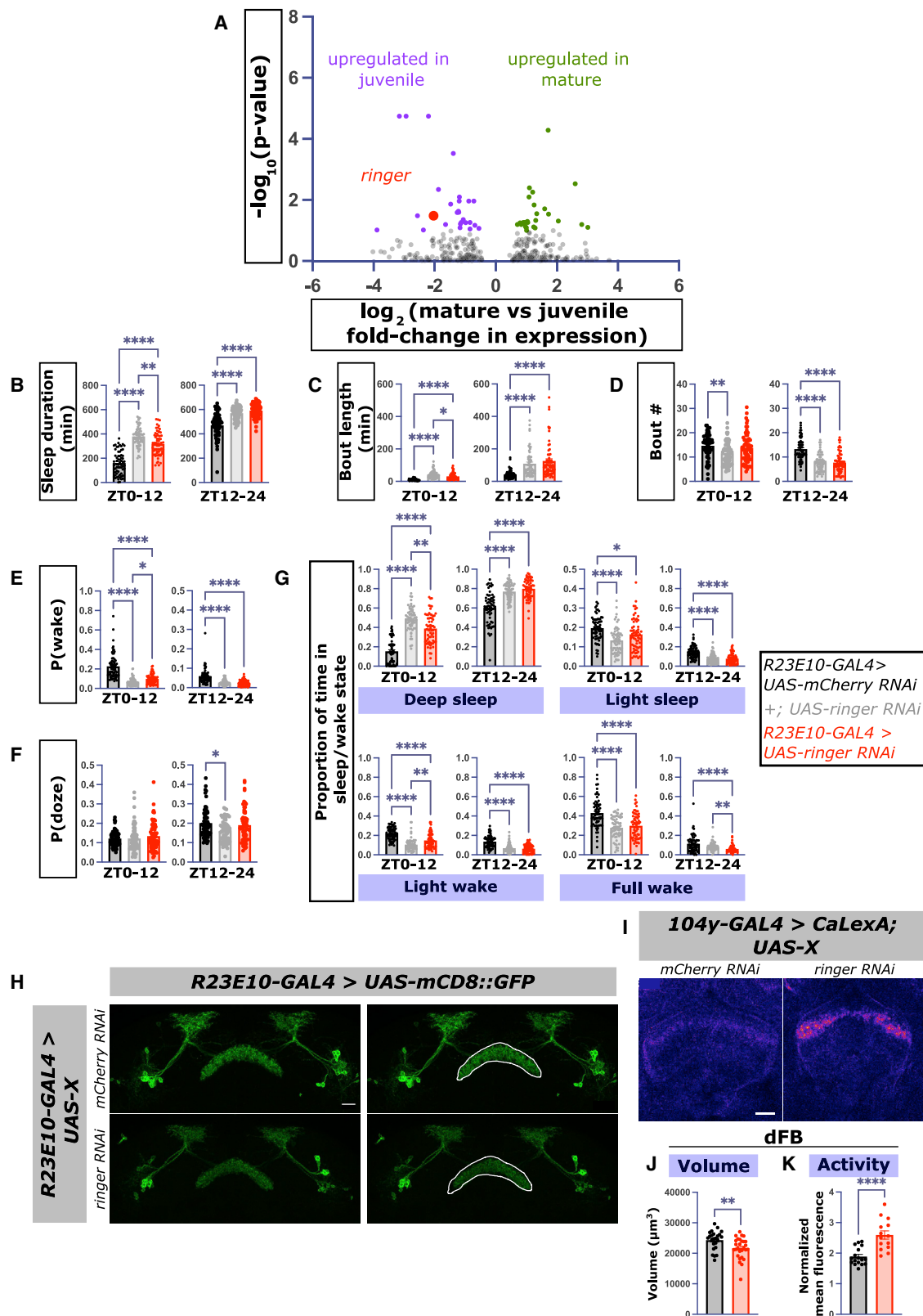


Figure 7. *Ringer* is involved in behavioral sleep maturation and the development of sleep-promoting dFB neurons

(A) DEGs based on published datasets.³⁷ Purple, genes that are more highly expressed in juvenile versus mature flies; green, genes that are more highly expressed in mature versus juvenile flies; red, *ringer* expression in mature versus juvenile flies, based on an adjusted p value cutoff ($p\text{-adj} > 0.1$).

(legend continued on next page)

- RNAi-based ontogeny screen of differentially expressed dFB genes
- Immunohistochemistry
- Imaging and analysis
- **QUANTIFICATION AND STATISTICAL ANALYSIS**

SUPPLEMENTAL INFORMATION

Supplemental information can be found online at <https://doi.org/10.1016/j.cub.2022.07.054>.

ACKNOWLEDGMENTS

We thank members of the Kayser Lab, Raizen Lab, Leela Chakravarti Dilley, and members of the Penn Chronobiology and Sleep Institute for helpful discussions/input. We thank Leslie Griffith and Timothy Wiggin for assisting with the custom MATLAB codes used for sleep/wake transition probabilities and HMM of sleep/wake substates. This work was supported by NIH grants DP2NS111996, R56NS109144, and R01NS120979 to M.S.K.; T32HL07953 to N.N.G.; and R21MH123841 and R01AG071818 to R.B. Additional funding was from the Burroughs Wellcome Career Award for Medical Scientists to M.S.K., the 2020 Max Planck Humboldt Research Award to R.B., and NSF grant CPS2038873 and the Honda Research Institute to K.S.

AUTHOR CONTRIBUTIONS

Conceptualization, N.N.G. and M.S.K.; investigation, N.N.G., H.N.B.L., A.H.D., B.M., E.S., K.S., and R.B.; writing – original draft, N.N.G. and M.S.K.; writing – review & editing, all authors; project supervision and funding, M.S.K.

DECLARATION OF INTERESTS

The authors declare no competing interests.

Received: November 4, 2021

Revised: June 6, 2022

Accepted: July 21, 2022

Published: August 18, 2022

REFERENCES

1. Kayser, M.S., and Biron, D. (2016). Sleep and development in genetically tractable model organisms. *Genetics* 203, 21–33.
2. Kayser, M.S., Yue, Z., and Sehgal, A. (2014). A critical period of sleep for development of courtship circuitry and behavior in *Drosophila*. *Science* 344, 269–274.
3. Dilley, L.C., Vigderman, A., Williams, C.E., and Kayser, M.S. (2018). Behavioral and genetic features of sleep ontogeny in *Drosophila*. *Sleep* 41, zsy086.
4. Roffwarg, H.P., Muzio, J.N., and Dement, W.C. (1966). Ontogenetic development of the human sleep-dream cycle. *Science* 152, 604–619.
5. Jouvet-Mounier, D., Astic, L., and Lacote, D. (1969). Ontogenesis of the states of sleep in rat, cat, and guinea pig during the first postnatal month. *Dev. Psychobiol.* 2, 216–239.
6. Seugnet, L., Suzuki, Y., Donlea, J.M., Gottschalk, L., and Shaw, P.J. (2011). Sleep deprivation during early-adult development results in long-lasting learning deficits in adult *Drosophila*. *Sleep* 34, 137–146.
7. Jones, C.E., Opel, R.A., Kaiser, M.E., Chau, A.Q., Quintana, J.R., Nipper, M.A., Finn, D.A., Hammock, E.A.D., and Lim, M.M. (2019). Early-life sleep disruption increases parvalbumin in primary somatosensory cortex and impairs social bonding in prairie voles. *Sci. Adv.* 5, eaav5188.
8. Cao, J., Herman, A.B., West, G.B., Poe, G., and Savage, V.M. (2020). Unraveling why we sleep: quantitative analysis reveals abrupt transition from neural reorganization to repair in early development. *Sci. Adv.* 6, eaba0398.
9. Marks, G.A., Shaffery, J.P., Oksenberg, A., Speciale, S.G., and Roffwarg, H.P. (1995). A functional role for REM sleep in brain maturation. *Behav. Brain Res.* 69, 1–11.
10. Blumberg, M.S. (2015). Developing sensorimotor systems in our sleep. *Curr. Dir. Psychol. Sci.* 24, 32–37.
11. Frank, M.G., Issa, N.P., and Stryker, M.P. (2001). Sleep enhances plasticity in the developing visual cortex. *Neuron* 30, 275–287.
12. Eban-Rothschild, A., Appelbaum, L., and de Lecea, L. (2018). Neuronal mechanisms for sleep/wake regulation and modulatory drive. *Neuropsychopharmacology* 43, 937–952.
13. Scammell, T.E., Arrigoni, E., and Lipton, J.O. (2017). Neural circuitry of wakefulness and sleep. *Neuron* 93, 747–765.
14. Artiushin, G., and Sehgal, A. (2017). The *Drosophila* circuitry of sleep-wake regulation. *Curr. Opin. Neurobiol.* 44, 243–250.
15. Blake, H., and Gerard, R.W. (1937). Brain potentials during sleep. *Am. J. Physiol.-Legacy Content* 119, 692–703.
16. Nitz, D.A., van Swinderen, B., Tononi, G., and Greenspan, R.J. (2002). Electrophysiological correlates of rest and activity in *Drosophila melanogaster*. *Curr. Biol.* 12, 1934–1940.
17. Yap, M.H.W., Grabowska, M.J., Rohrscheib, C., Jeans, R., Troup, M., Paulk, A.C., van Alphen, B., Shaw, P.J., and van Swinderen, B. (2017). Oscillatory brain activity in spontaneous and induced sleep stages in flies. *Nat. Commun.* 8, 1815.
18. Tainton-Heap, L.A.L., Kirszenblat, L.C., Notaras, E.T., Grabowska, M.J., Jeans, R., Feng, K., Shaw, P.J., and van Swinderen, B. (2021). A paradoxical kind of sleep in *Drosophila melanogaster*. *Curr. Biol.* 31, 578–590.e6.
19. Lendner, J.D., Helfrich, R.F., Mander, B.A., Romundstad, L., Lin, J.J., Walker, M.P., Larsson, P.G., and Knight, R.T. (2020). An electrophysiological marker of arousal level in humans. *eLife* 9, e55092.
20. Yamabe, M., Horie, K., Shiokawa, H., Funato, H., Yanagisawa, M., and Kitagawa, H. (2019). MC-SleepNet: large-scale sleep stage scoring in mice by deep neural networks. *Sci. Rep.* 9, 15793.
21. Clancy, J.J., Caldwell, D.F., Villeneuve, M.J., and Sangiiah, S. (1978). Daytime sleep-wake cycle in the rat. *Physiol. Behav.* 21, 457–459.
22. Weber, F. (2017). Modeling the mammalian sleep cycle. *Curr. Opin. Neurobiol.* 46, 68–75.

(B–G) Total sleep duration (B), bout length (C), bout number (D), P(wake) (E), P(doze) (F), and proportion of time spent in deep sleep, light sleep, light wake, and full wake (G) between ZT0–12 and ZT12–24 in *R23E10-GAL4>UAS-ringer RNAi* (red, n = 63) compared with *R23E10-GAL4>UAS-mCherry RNAi* (black, n = 64) and +; *UAS-ringer RNAi* controls (gray, n = 63) (Kruskall-Wallis with post hoc Dunn’s multiple comparison tests).

(H) Representative images of maximum intensity projections of z stacks used to quantify *R23E10-GAL4* projection volume in the dFB in *R23E10-GAL4>UAS-mCherry RNAi* controls (top) and *R23E10-GAL4>UAS-ringer RNAi*. White outlines on the right denote the borders of dFB projections in *R23E10-GAL4>UAS-mCherry RNAi* control flies.

(I) Representative optical sections used to quantify dFB activity in *104y-GAL4>CaLexA; UAS-mCherry RNAi* controls (left) and *104y-GAL4>CaLexA; UAS-ringer RNAi* flies (right).

(J and K) Quantified dFB volume (J) and activity (K) in controls (black) and in the setting of *ringer* knockdown (red). From left to right: n = 24, 28, 17, and 14 brains (Mann-Whitney tests). Scale bars, 20 μ m.

For all graphs in this figure and other figures, data are presented as mean \pm SEM. Significance values within figures are denoted as follows: *p < 0.05, **p < 0.01, ***p < 0.001, ****p < 0.0001. See also [Figure S7](#) and [Tables S1–S3](#).

23. Wiggan, T.D., Goodwin, P.R., Donelson, N.C., Liu, C., Trinh, K., Sanyal, S., and Griffith, L.C. (2020). Covert sleep-related biological processes are revealed by probabilistic analysis in *Drosophila*. *Proc. Natl. Acad. Sci. USA* *117*, 10024–10034.
24. Liu, Q., Liu, S., Kodama, L., Driscoll, M.R., and Wu, M.N. (2012). Two dopaminergic neurons signal to the dorsal fan-shaped body to promote wakefulness in *Drosophila*. *Curr. Biol.* *22*, 2114–2123.
25. Pimentel, D., Donlea, J.M., Talbot, C.B., Song, S.M., Thurston, A.J.F., and Miesenböck, G. (2016). Operation of a homeostatic sleep switch. *Nature* *536*, 333–337.
26. Ueno, T., Tomita, J., Tanimoto, H., Endo, K., Ito, K., Kume, S., and Kume, K. (2012). Identification of a dopamine pathway that regulates sleep and arousal in *Drosophila*. *Nat. Neurosci.* *15*, 1516–1523.
27. Chakravarti Dilley, L., Szuperak, M., Gong, N.N., Williams, C.E., Saldana, R.L., Garbe, D.S., Syed, M.H., Jain, R., and Kayser, M.S. (2020). Identification of a molecular basis for the juvenile sleep state. *eLife* *9*, e52676.
28. Shaw, P.J., Cirelli, C., Greenspan, R.J., and Tononi, G. (2000). Correlates of sleep and waking in *Drosophila melanogaster*. *Science* *287*, 1834–1837.
29. Isaac, R.E., Li, C., Leedale, A.E., and Shirras, A.D. (2010). *Drosophila* male sex peptide inhibits siesta sleep and promotes locomotor activity in the post-mated female. *Proc. Biol. Sci.* *277*, 65–70.
30. Garbe, D.S., Vigderman, A.S., Moscato, E., Dove, A.E., Vecsey, C.G., Kayser, M.S., and Sehgal, A. (2016). Changes in female *Drosophila* sleep following mating are mediated by SPSN-SAG neurons. *J. Biol. Rhythms* *31*, 551–567.
31. Donlea, J.M., Pimentel, D., and Miesenböck, G. (2014). Neuronal machinery of sleep homeostasis in *Drosophila*. *Neuron* *81*, 1442.
32. Donlea, J.M., Pimentel, D., Talbot, C.B., Kempf, A., Omoto, J.J., Hartenstein, V., and Miesenböck, G. (2018). Recurrent circuitry for balancing sleep need and sleep. *Neuron* *97*, 378–389.e4.
33. Hamada, F.N., Rosenzweig, M., Kang, K., Pulver, S.R., Ghezzi, A., Jegla, T.J., and Garrity, P.A. (2008). An internal thermal sensor controlling temperature preference in *Drosophila*. *Nature* *454*, 217–220.
34. McGuire, S.E., Mao, Z., and Davis, R.L. (2004). Spatiotemporal gene expression targeting with the TARGET and gene-switch systems in *Drosophila*. *Sci. STKE* *2004*, pl6.
35. Qian, Y., Cao, Y., Deng, B., Yang, G., Li, J., Xu, R., Zhang, D., Huang, J., and Rao, Y. (2017). Sleep homeostasis regulated by 5HT2B receptor in a small subset of neurons in the dorsal fan-shaped body of *Drosophila*. *eLife* *6*, e26519.
36. Troup, M., Yap, M.H., Rohrscheib, C., Grabowska, M.J., Ertekin, D., Randeniya, R., Kottler, B., Larkin, A., Munro, K., Shaw, P.J., et al. (2018). Acute control of the sleep switch in *Drosophila* reveals a role for gap junctions in regulating behavioral responsiveness. *eLife* *7*, e37105.
37. Davie, K., Janssens, J., Koldere, D., De Waegeneer, M., Pech, U., Kreft, L., Aibar, S., Makhzami, S., Christiaens, V., Bravo González-Blas, C., et al. (2018). A single-cell transcriptome atlas of the aging *Drosophila* brain. *Cell* *174*, 982–998.e20.
38. Subramanian, A., Tamayo, P., Mootha, V.K., Mukherjee, S., Ebert, B.L., Gillette, M.A., Paulovich, A., Pomeroy, S.L., Golub, T.R., Lander, E.S., et al. (2005). Gene set enrichment analysis: a knowledge-based approach for interpreting genome-wide expression profiles. *Proc. Natl. Acad. Sci. USA* *102*, 15545–15550.
39. Mootha, V.K., Lindgren, C.M., Eriksson, K.-F., Subramanian, A., Sihag, S., Lehar, J., Puigserver, P., Carlsson, E., Ridderstråle, M., Laurila, E., et al. (2003). PGC-1 α -responsive genes involved in oxidative phosphorylation are coordinately downregulated in human diabetes. *Nat. Genet.* *34*, 267–273.
40. Mino, R.E., Rogers, S.L., Risinger, A.L., Rohena, C., Banerjee, S., and Bhat, M.A. (2016). *Drosophila* Ringmaker regulates microtubule stabilization and axonal extension during embryonic development. *J. Cell Sci.* *129*, 3282–3294.
41. Vargas, E.J.M., Matamoros, A.J., Qiu, J., Jan, C.H., Wang, Q., Gorczyca, D., Han, T.W., Weissman, J.S., Jan, Y.N., Banerjee, S., et al. (2020). The microtubule regulator ringer functions downstream from the RNA repair/splicing pathway to promote axon regeneration. *Genes Dev.* *34*, 194–208.
42. Masuyama, K., Zhang, Y., Rao, Y., and Wang, J.W. (2012). Mapping neural circuits with activity-dependent nuclear import of a transcription factor. *J. Neurogenet.* *26*, 89–102.
43. Knoop, M.S., de Groot, E.R., and Dudink, J. (2021). Current ideas about the roles of rapid eye movement and non-rapid eye movement sleep in brain development. *Acta Paediatr.* *110*, 36–44.
44. Dumoulin Bridi, M.C.D., Aton, S.J., Seibt, J., Renouard, L., Coleman, T., and Frank, M.G. (2015). Rapid eye movement sleep promotes cortical plasticity in the developing brain. *Sci. Adv.* *1*, e1500105.
45. Shaffery, J.P., Sinton, C.M., Bissette, G., Roffwarg, H.P., and Marks, G.A. (2002). Rapid eye movement sleep deprivation modifies expression of long-term potentiation in visual cortex of immature rats. *Neuroscience* *110*, 431–443.
46. Li, W., Ma, L., Yang, G., and Gan, W.-B. (2017). REM sleep selectively prunes and maintains new synapses in development and learning. *Nat. Neurosci.* *20*, 427–437.
47. Blumberg, M.S., Marques, H.G., and Iida, F. (2013). Twitching in sensorimotor development from sleeping rats to robots. *Curr. Biol.* *23*, R532–R537.
48. Mohns, E.J., and Blumberg, M.S. (2010). Neocortical activation of the hippocampus during sleep in infant rats. *J. Neurosci.* *30*, 3438–3449.
49. Sokoloff, G., Dooley, J.C., Glanz, R.M., Wen, R.Y., Hickerson, M.M., Evans, L.G., Laughlin, H.M., Apfelbaum, K.S., and Blumberg, M.S. (2021). Twitches emerge postnatally during quiet sleep in human infants and are synchronized with sleep spindles. *Curr. Biol.* *31*, 3426–3432.e4.
50. Tononi, G., and Cirelli, C. (2006). Sleep function and synaptic homeostasis. *Sleep Med. Rev.* *10*, 49–62.
51. Kurth, S., Ringli, M., Geiger, A., LeBourgeois, M., Jenni, O.G., and Huber, R. (2010). Mapping of cortical activity in the first two decades of life: a high-density sleep electroencephalogram study. *J. Neurosci.* *30*, 13211–13219.
52. Lindersson, E., Lundvig, D., Petersen, C., Madsen, P., Nyengaard, J.R., Højrup, P., Moos, T., Otzen, D., Gai, W.-P., Blumberg, P.C., et al. (2005). p25 α stimulates α -synuclein aggregation and is co-localized with aggregated α -synuclein in α -Synucleinopathies*. *J. Biol. Chem.* *280*, 5703–5715.
53. Xie, J., Chen, S., Bopassa, J.C., and Banerjee, S. (2021). *Drosophila* tubulin polymerization promoting protein mutants reveal pathological correlates relevant to human Parkinson's disease. *Sci. Rep.* *11*, 13614.
54. Iourov, I.Y.u., Vorsanova, S.G., Saprina, E.A., and Yurov, Y.u.B. (2010). Identification of candidate genes of autism on the basis of molecular cytogenetic and in silico studies of the genome organization of chromosomal regions involved in unbalanced rearrangements. *Russ. J. Genet.* *46*, 1190–1193.
55. Love, M.I., Huber, W., and Anders, S. (2014). Moderated estimation of fold change and dispersion for RNA-seq data with DESeq2. *Genome Biol.* *15*, 550.
56. Powell, J.A.C. (2014). GO2MSIG, an automated GO based multi-species gene set generator for gene set enrichment analysis. *BMC Bioinformatics* *15*, 146.
57. Ni, J.-Q., Zhou, R., Czech, B., Liu, L.-P., Holderbaum, L., Yang-Zhou, D., Shim, H.-S., Tao, R., Handler, D., Karpowicz, P., et al. (2011). A genome-scale shRNA resource for transgenic RNAi in *Drosophila*. *Nat. Methods* *8*, 405–407.

STAR★METHODS

KEY RESOURCES TABLE

REAGENT or RESOURCE	SOURCE	IDENTIFIER
Antibodies		
rabbit anti-GFP antibody	Invitrogen	Cat#A11122; RRID: AB_221569
donkey anti-rabbit AlexaFluor488 antibody	ThermoFisher	Cat#A21206; RRID: AB_2535792
Deposited data		
Single-cell RNASeq of <i>Drosophila</i> brains	Davie et al. ³⁷	GEO: GSE107451 (https://www.ncbi.nlm.nih.gov/geo/query/acc.cgi?acc=GSE107451)
Experimental models: Organisms/strains		
<i>D. melanogaster</i> : Iso31 strain	Laboratory stock	N/A
<i>D. melanogaster</i> : Canton-S strain	Laboratory stock	N/A
<i>D. melanogaster</i> : w ¹¹¹⁸ strain	Laboratory stock	N/A
<i>D. melanogaster</i> : UAS- <i>dTrpA1</i>	Gift from Dr. Leslie Griffith (Brandeis University)	N/A
<i>D. melanogaster</i> : R23E10-GAL4: P{y[+7.7] w[+mC]=GMR23E10-GAL4}attP2	Bloomington Drosophila Stock Center	BDSC#49032; FlyBase: FBti0134066
<i>D. melanogaster</i> : UAS- <i>Kir2.1-GFP</i> : P{w[+mC]=UAS-Hsap\KCNJ2.EGFP}7	Bloomington Drosophila Stock Center	BDSC#6595; FlyBase: FBti0017552
<i>D. melanogaster</i> : mCherry RNAi control for TRiP lines: y[1] sc[*] v[1] sev[21]; P{y[+7.7] v[+t1.8]=UAS-mCherry.VALIUM10}attP2	Bloomington Drosophila Stock Center	BDSC#35787; FlyBase: FBti0143387
<i>D. melanogaster</i> : RNAi for <i>pdm3</i> : y[1] v[1]; P{y[+7.7] v[+t1.8]=TRiP.HMJ21205}attP40	Bloomington Drosophila Stock Center	BDSC#53887; Flybase: FBti0158267
<i>D. melanogaster</i> : RNAi for <i>ringer</i> : y[1] sc[*] v[1] sev[21]; P{y[+7.7] v[+t1.8]=TRiP.HMS01740}attP40	Bloomington Drosophila Stock Center	BDSC#38287; Flybase: FBti0149487
Software and algorithms		
Sleep/wake transition probabilities and hidden Markov modeling of sleep substates	Wiggin et al. ²³	https://github.com/Griffith-Lab/Fly_Sleep_Probability
DESeq2	Love et al. ⁵⁵	http://www.bioconductor.org/packages/release/bioc/html/DESeq2.html
Gene Set Enrichment Analysis	Subramanian et al. ³⁸	https://www.gsea-msigdb.org/
Gene set collections for gene ontology annotations	Powell et al. ⁵⁶	http://www.bioinformatics.org/go2msig/releases/
Other		
<i>Drosophila</i> Activity Monitoring system	Trikinetics	Single-beam DAM system, DAM5H multibeam system

RESOURCE AVAILABILITY

Lead contact

Further information and requests for resources and reagents should be directed to and will be fulfilled by the lead contact, Matthew Kayser (kayser@pennterapeutics.com).

Materials availability

This study did not generate new unique reagents.

Data and code availability

- This paper analyzes existing, publicly available data. The accession numbers for the datasets are listed in the [key resources table](#).

- This paper does not report original code.
- Any additional information required to reanalyze the data reported in this paper is available from the lead contact upon request.

EXPERIMENTAL MODEL AND SUBJECT DETAILS

Drosophila melanogaster were raised and maintained on standard molasses food (8.0% molasses, 0.55% agar, 0.2% Tegosept, 0.5% propionic acid) at 25°C on a 12hr:12hr light:dark cycle. Female flies were used in all experiments.

METHOD DETAILS

Sleep assays

For ontogeny experiments unless otherwise specified, newly-eclosed female flies were collected and aged in group housing on standard food. Juvenile flies were collected on the day of eclosion and loaded into the DAM system between ZT4-6, along with mature flies aged 5-9 days post-eclosion. Unless otherwise specified, sleep assays were run at 25°C on a 12-hour/12-hour light/dark schedule.

Thermogenetic activation and inhibition experiments

Animals were raised at 18°C to prevent TrpA1 activation or Kir2.1 expression during development. For TrpA1 activation experiments, adult female flies were collected at eclosion and aged at 18°C on standard fly food. 5-9 day old flies were loaded into the DAM system to monitor sleep and placed at 22°C on a 12:12: LD schedule for 3 days. TrpA1 activation was performed by a temperature shift to 31°C across non-consecutive 12-hour light or 12-hour dark periods. Between increases in temperature, flies were maintained at 22°C. For Kir2.1 inhibition experiments, adult female flies were collected at eclosion and aged at 18°C in group-housed conditions. Juvenile flies were collected at eclosion from ZT4-6 and loaded into the DAM system along with 5-9 day old flies at 31°C.

Sleep/wake transition probabilities and hidden Markov modeling analysis

P(wake) and P(doze) were calculated from 1-minute bins of activity collected in the DAM system in Matlab as previously described.²³ Hidden Markov modeling of sleep/wake substates was constrained with parameters as previously described:²³ a transition from deep sleep to full wake could only do so through light wake, while a transition from full wake to deep sleep could only do so through light sleep. HMMs were trained on the transitions (wake or doze) between 1-minute bins of activity (for 24 hours, 1439 transitions per fly). HMM fitting and hidden state analysis was performed as previously described using the Matlab Statistics and Machine Learning Toolkit.²³ For characterizing ontogenetic differences in juvenile vs mature *iso31* fly sleep/wake substates (Figure 1 and associated supplemental figures), HMMs were trained based on transitions as measured using the DAM5H multibeam system (Trikinetics) (Tables S1A and S1B). For experiments involving *Canton-S* and *w¹¹¹⁸* flies, HMMs were trained based on transitions as measured in mature *Canton-S* or *w¹¹¹⁸* flies using the DAM5H multibeam system (Tables S1C and S1D). For *iso31* sleep deprivation experiments (Figure 3) and *R23E10-GAL4+* neuron functional manipulations (Figures 4 and 5), an HMM was trained on mature *iso31* activity transitions measured using the single beam DAM system (Trikinetics) (Table S1E). For *pdm3* knockdown experiments, an HMM was trained on mature *elav-GAL4; + (attP40)* activity transitions measured using the single beam DAM system (Table S1F). A separate HMM was trained on activity transitions measured using the multibeam DAM system from all *R23E10-GAL4>UAS-mCherry RNAi* flies for assessing sleep/wake substates in the setting of *R23E10-GAL4* driven RNAi knockdown (Table S1G). Trained HMMs were used to calculate the proportion of time spent in sleep/wake hidden states.

Single cell RNA-Seq analysis

Using published single-cell data from *Drosophila* brains, cells annotated as dFB neurons were extracted from previously performed clustering³⁷ (cluster 61 in the 57K dataset with clustering resolution 2.0) and collapsed into pseudobulk transcriptomes per replicate. Differential expression comparing young (d0 or d1 flies) vs old (d9 flies) was performed on both sets of pseudobulk transcriptomes using DESeq2.⁵⁵ Genes significantly differentially expressed ($p\text{-adj} < 0.1$) formed the candidate list for the RNAi-based screen.

Gene set enrichment analysis of differentially expressed dFB genes

Gene set collections for Gene Ontology annotations were downloaded from public sources.⁵⁶ To compare DEGs upregulated in mature or juvenile flies, a gene signature was generated by ranking all DEGs with $p\text{-adj} > 0.1$ according to DESeq2-derived test statistics. Enrichment analysis was performed with GSEA v4.0³⁸ using weighted statistical analysis. Gene sets with a false discovery rate < 0.25 were considered significantly enriched.

RNAi-based ontogeny screen of differentially expressed dFB genes

Virgin collected from the *R23E10-GAL4* fly stock were crossed to males of RNAi fly stocks from the Transgenic RNAi Project (TRiP) collection.⁵⁷ We utilized all available VALIUM10, VALIUM20, or VALIUM22 lines for a given gene (Table S3). For controls, we used *R23E10-GAL4 x UAS-mCherry RNAi* and *iso31 x UAS-RNAi*. Sleep ontogeny assays were performed as described above. The multibeam DAM system was used to collect 1-minute bins of activity for calculating sleep/wake transition probabilities and HMM hidden states.

Immunohistochemistry

Fly brains were dissected in 1xPBS and fixed in 4% PFA in PBS with 0.3% Triton-X 100 (PBST) for 20 minutes at room temperature. For experiments involving CaLexA, brains were dissected at ZT8. Following 3x10 minute washes in PBST, brains were incubated overnight at 4°C with rabbit anti-GFP primary antibody (Invitrogen, Cat# A11122) at 1:500 dilution. Brains were washed 3x10 minutes in PBST, and incubated in donkey anti-rabbit Alexa Fluor 488 (Thermo Fisher) at 1:250 for 2 hours at room temperature. After 3x10 minute washes in PBST, brains were cleared in 50% glycerol and mounted in Vectashield.

Imaging and analysis

Images were taken using a Leica TCS SP8 confocal microscope and processed in NIH Fiji. All settings were kept constant between conditions within a given experiment. Images were taken in 1.0µm steps. To quantify *R23E10-GAL4* projection volume to the dFB, for each Z-slice, *R23E10-GAL4* dFB projections were manually outlined. The full volume of the projections was measured using the 3D Objects counter function in Fiji with the following settings: threshold = 1 and minimum puncta size = 100. For experiments involving CaLexA, single optical sections were selected from a z-stack. The dFB was manually outlined. Mean GFP fluorescence was measured from this selection and normalized to mean fluorescence from the background, which was chosen as a consistently-sized square area in the ventral FB (normalized fluorescence = dFB mean fluorescence / mean background fluorescence). Imaging and analysis were done blind to experimental condition.

QUANTIFICATION AND STATISTICAL ANALYSIS

All statistical analyses were performed using GraphPad Prism (version 8.4.1). For all figures, data are presented as mean ± SEM. Significance values within figures are denoted as follows: **P* < 0.05, ***P* < 0.01, ****P* < 0.001, *****P* < 0.0001. For each experiment, the Shapiro-Wilk test was used to test for normality to determine usage of a parametric vs nonparametric statistical test. Sample sizes and specific tests are denoted in the figure legends. Means and/or median values, error values, and full statistical test results and tables are reported in [Data S1](#).

Current Biology, Volume 32

Supplemental Information

**Intrinsic maturation of sleep output neurons
regulates sleep ontogeny in *Drosophila***

Naihua N. Gong, Hang Ngoc Bao Luong, An H. Dang, Benjamin Mainwaring, Emily Shields, Karl Schmeckpeper, Roberto Bonasio, and Matthew S. Kayser

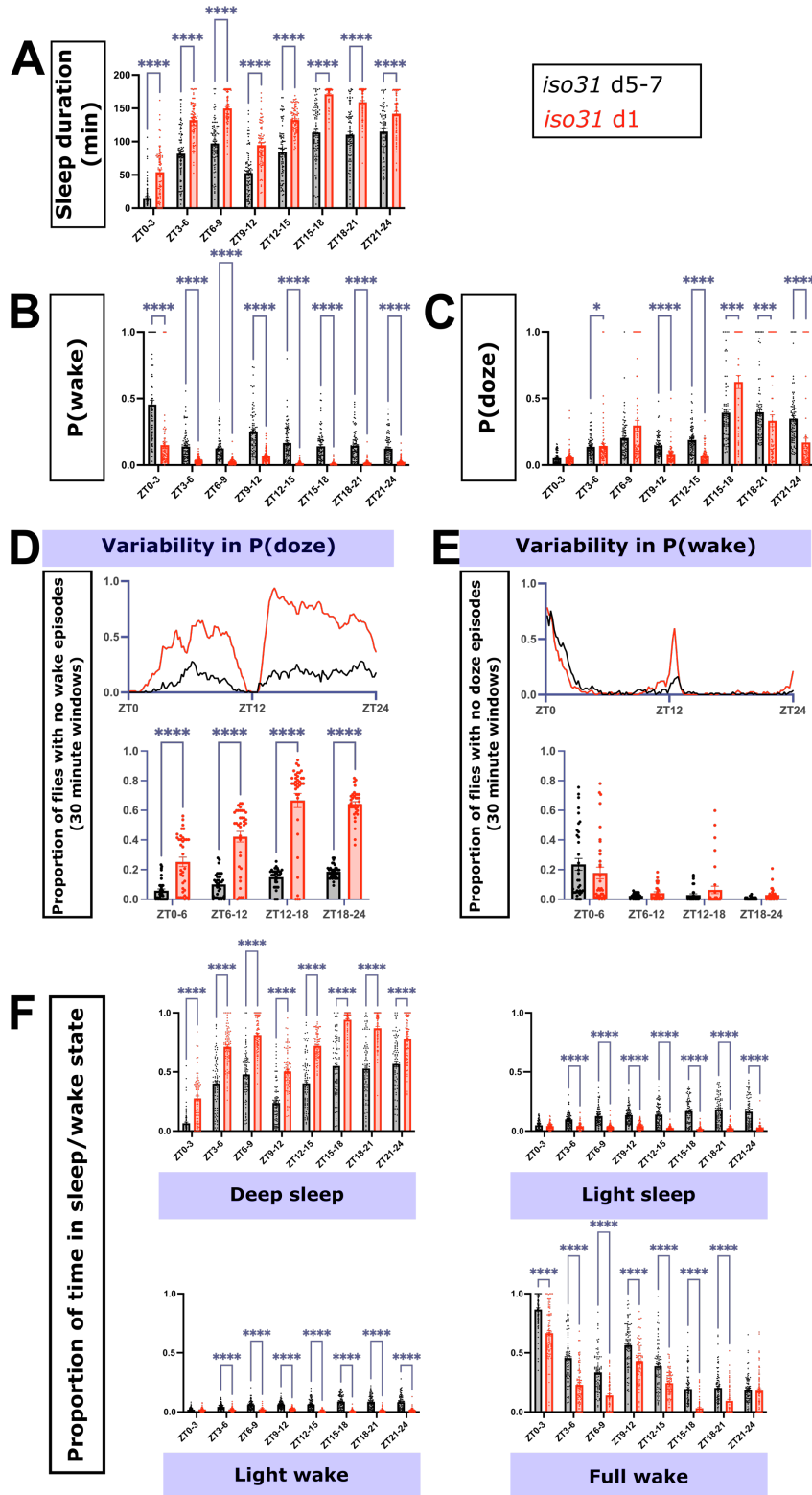
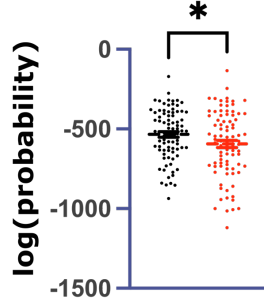
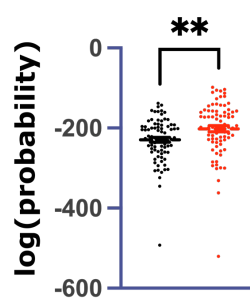


Figure S1: Sleep metrics of *iso31* flies binned in 3-hour intervals and P(doze) variability. Related to Figure 1. A) Sleep duration, B) P(wake), and C) P(doze) in mature (black, n = 87) and juvenile (red, n = 82) *iso31* flies binned into 3-hour intervals across 24 hours. Proportion of undefined D) P(doze) and E) P(wake) values across 24 hours in mature and juvenile flies shown in Figure 1 Top traces are a rolling 30-minute window sampled every 10 minutes, Bottom graphs show the average proportion of undefined values per 30-minute window across 6-hour intervals. (F) Proportion of time spent in deep sleep, light sleep, light wake, and full wake (Mann-Whitney U tests).

A *iso31* D5-7

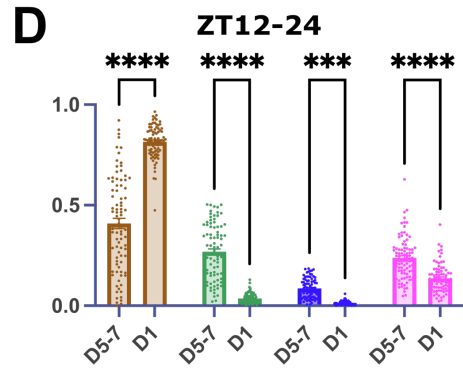
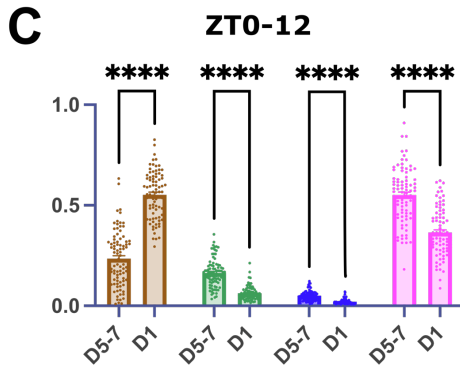


B *iso31* D1

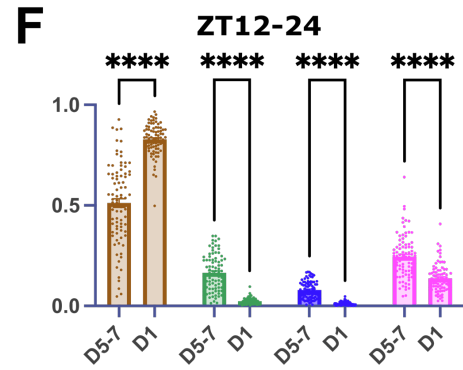
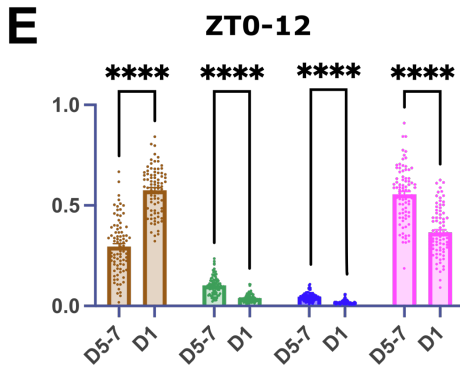


HMM-mature
HMM-juvenile

Applying HMM-mature:



Applying HMM-juvenile:



Proportion of time in sleep/wake state

Deep sleep Light wake
Light sleep Full wake

Figure S2: HMMs trained on mature vs juvenile *iso31* fly locomotor datasets.

Related to Figure 1. Log(probability) of observing a given sequence of locomotor behavior in A) mature or B) juvenile *iso31* flies by applying HMM-mature (black, n = 87) or HMM-juvenile (red, n = 82) (two-tailed T-tests). Proportion of time spent in each sleep/wake hidden state in mature vs juvenile flies from ZT0-12 and ZT12-24 when applying C, D) HMM-mature or E, F) HMM-juvenile (two-way ANOVA with post-hoc Sidak's multiple comparison test).

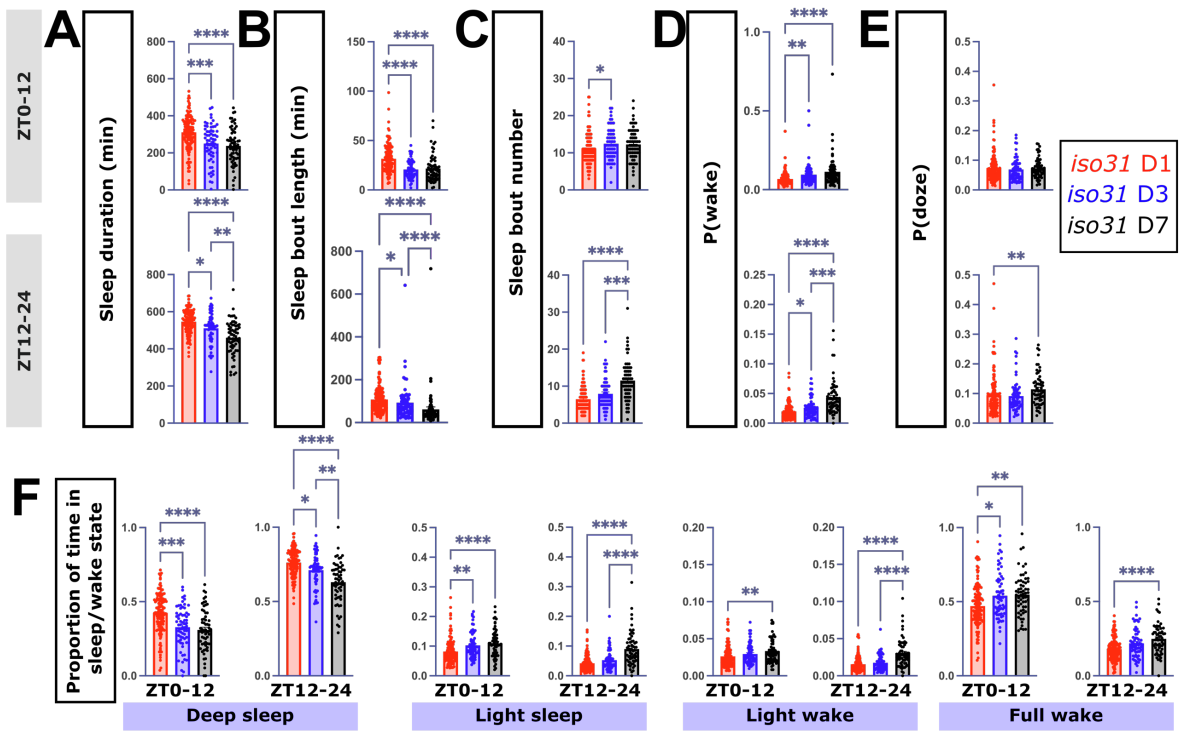


Figure S3: Developmental progression of sleep architecture and substates.

Related to Figure 1. A) Sleep duration, B) bout length, C) bout number, D) P(wake), and E) P(doze) in *iso31* flies at post-eclosion day 1 (red, n = 127), 3 (blue, n = 64), and 7 (black, n = 64) from ZT0-12 (top) and ZT12-24 (bottom). Proportion of time spent in F) deep sleep, light sleep, light wake, and full wake across the three age groups from ZT0-12 (left) and ZT12-24 (right) (Kruskall-Wallis with post-hoc Dunn's multiple comparison test).

iso31 d5-7
iso31 d1

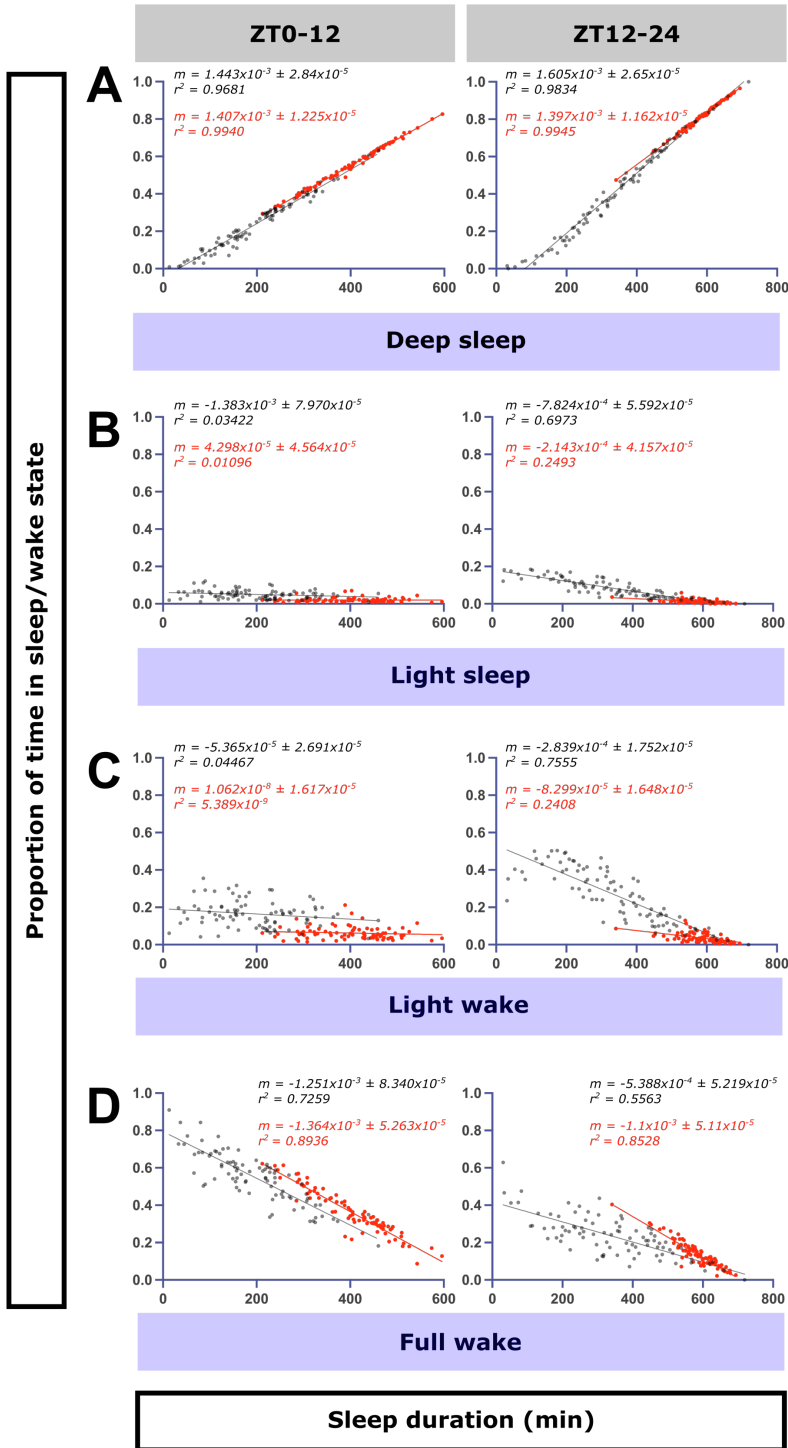


Figure S4: Correlation between sleep duration and proportion of time spent in a given sleep state. Related to Figure 1. Sleep duration vs proportion of time spent in A) deep sleep, B) light sleep, C) light wake, and D) full wake in individual mature (black) and juvenile *iso31* flies (red). The slope of the linear regressions are shown with \pm SEM, along with r^2 values, and color-coded according to the dataset used for the regression (mature or juvenile).

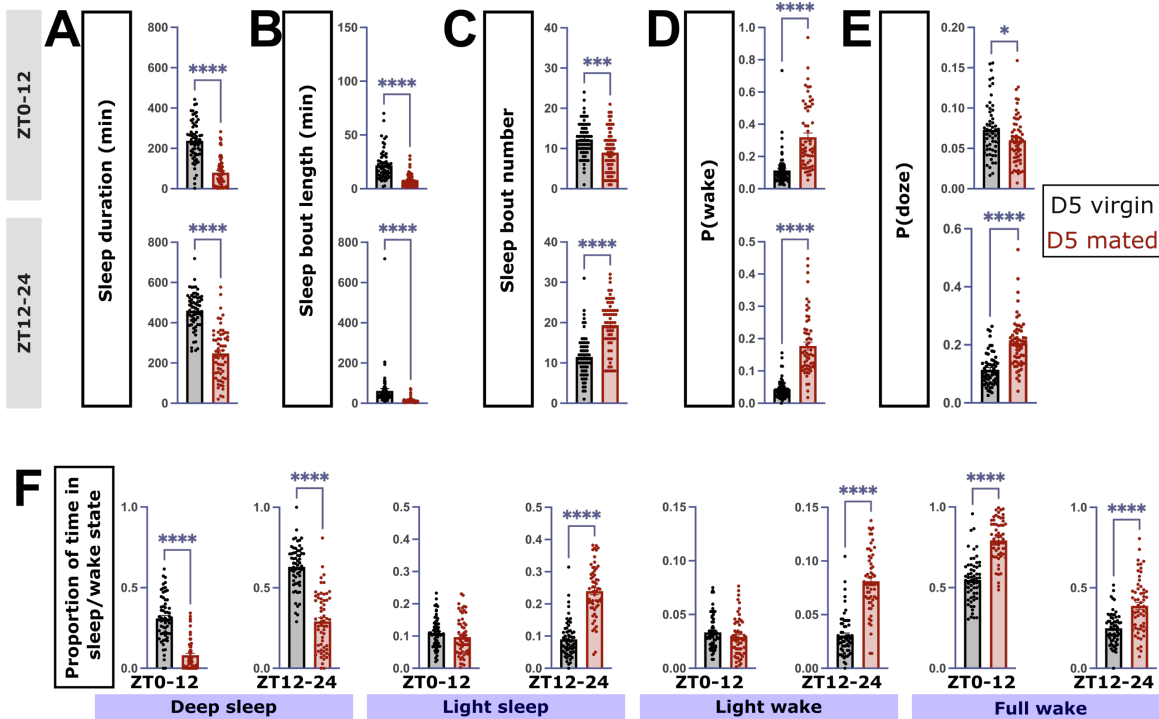


Figure S5: Mating status affects sleep architecture. Related to Figure 1. A)

Sleep duration, B) bout length, C) bout number, D) P(wake), and E) P(doze) in unmated (black, n = 64) and mated (maroon, n = 63) mature *iso31* flies from ZT0-12 (top) and ZT12-24 (bottom). Proportion of time spent in F) deep sleep, light sleep, light wake, and full wake in unmated vs mated flies from ZT0-12 (left) and ZT12-24 (right) (Mann-Whitney tests).

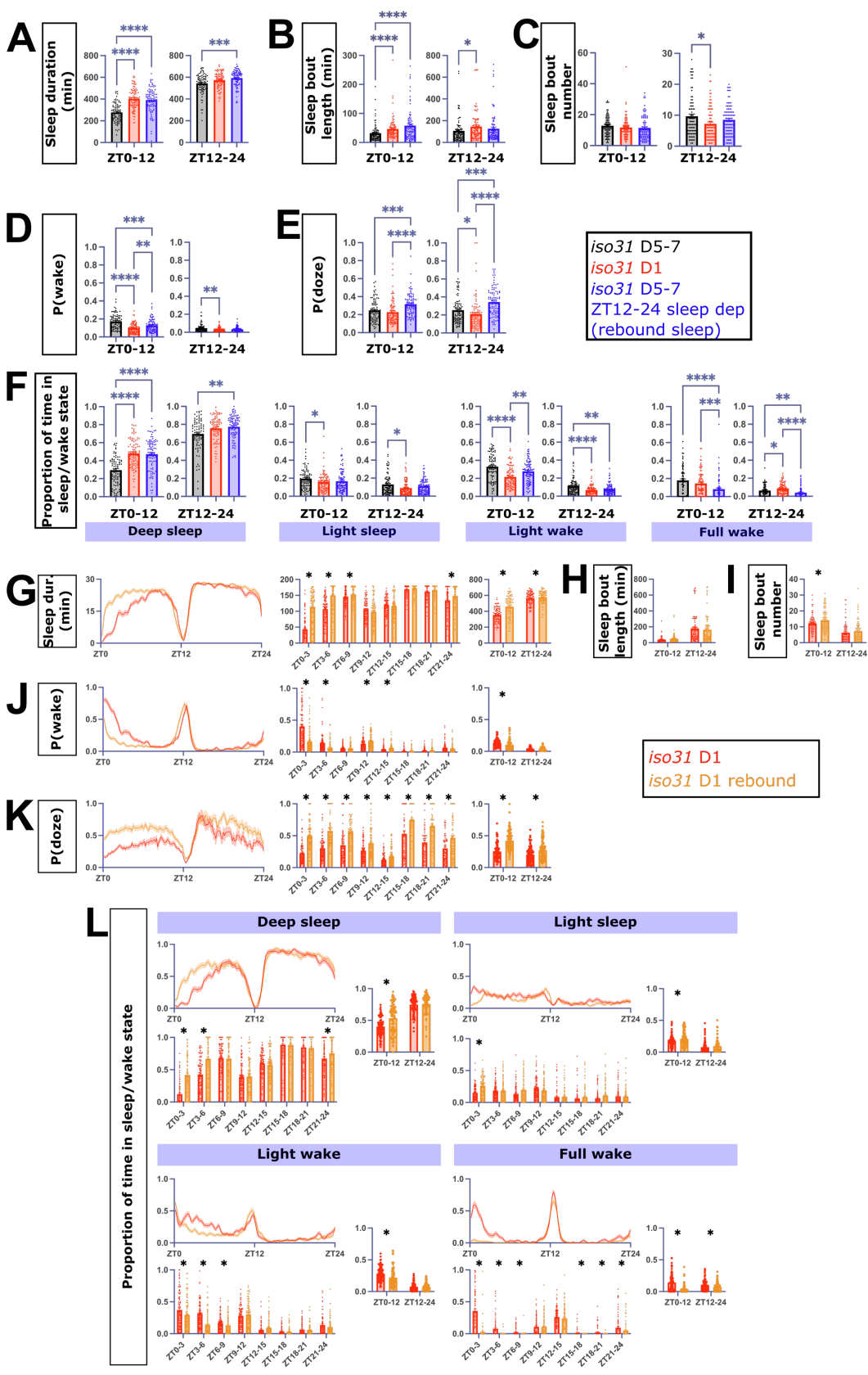
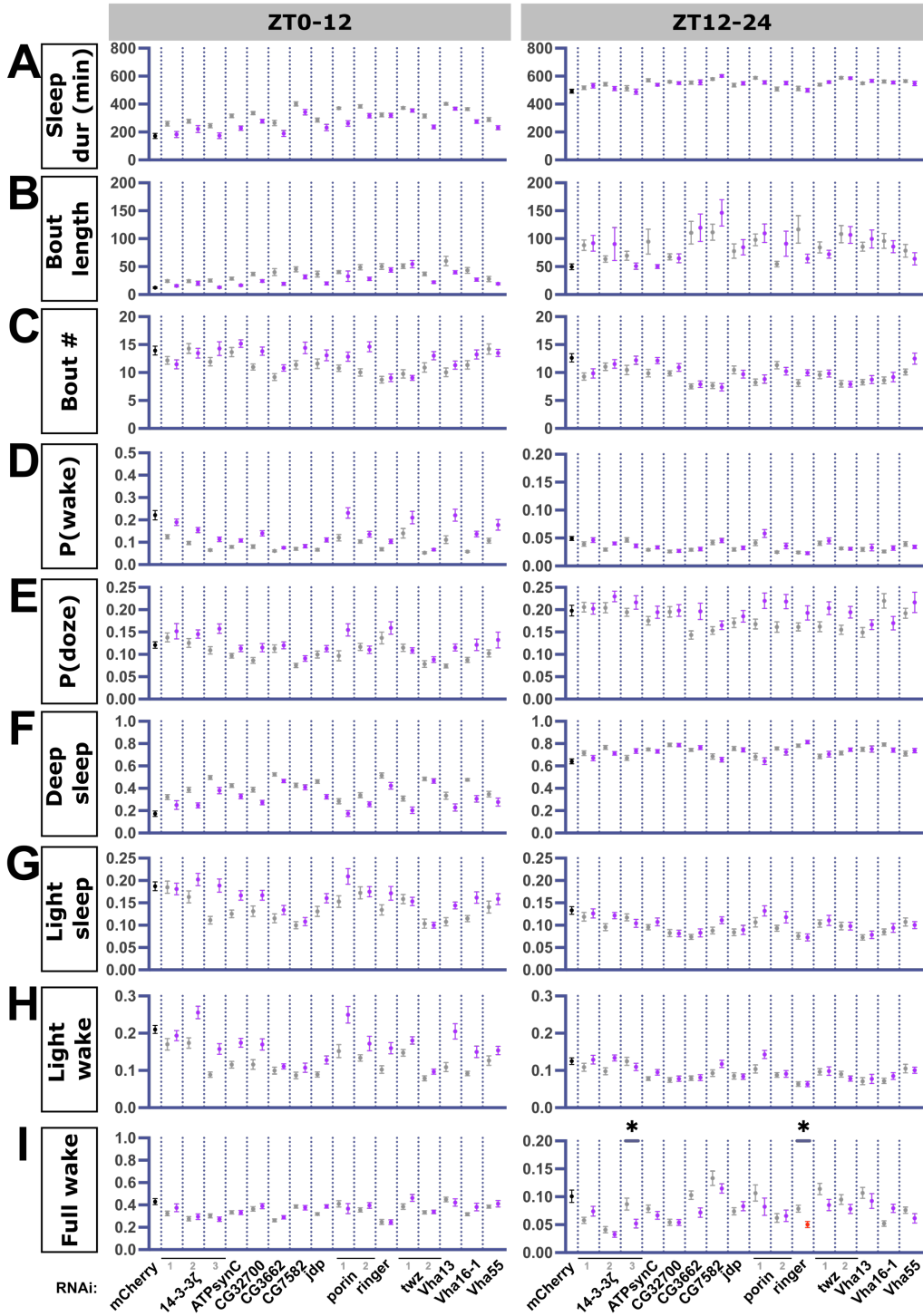


Figure S6: Extended sleep metrics after sleep deprivation in mature and juvenile flies. Related to Figure 3. A) Sleep duration, B) bout length, C) bout number, D) P(wake), and E) P(doze) in juvenile (red, n = 90), non-deprived control (black, n = 85), and mechanically sleep-deprived mature *iso31* flies (blue, n = 90) from ZT0-12 (left) and ZT12-24 (right). Proportion of time spent in F) deep sleep, light sleep, light wake, and full wake across the three conditions from ZT0-12 (left) and ZT12-24 (right) (Kruskall-Wallis with post-hoc Dunn's multiple comparison test for A-F). G) Sleep duration, H) bout length, I) bout number, J) P(wake), and K) P(doze) in non-deprived juvenile (orange, n = 92) and rebounding juvenile flies (light orange, n = 93). Proportion of time spent in L) deep sleep, light sleep, light wake, and full wake for all groups (Mann-Whitney tests for G-L).

R23E10-GAL4 > UAS-mCherry RNAi
 +; UAS-DEG RNAi
 R23E10-GAL4 > UAS-DEG RNAi
 R23E10-GAL4 > UAS-ringer RNAi



R23E10-GAL4 > UAS-RNAi

Figure S7: Sleep architecture metrics for *R23E10-GAL4>UAS-DEG RNAi* screen. Related to Figure 3. A) Sleep duration, B) sleep bout duration, C) sleep bout number, D) P(wake), E) P(doze), proportion of time spent in F) deep sleep, G) light sleep, H) light wake, and I) full wake in screened lines (*R23E10-GAL4>UAS-RNAi*, purple; *R23E10-GAL4>UAS-ringer RNAi*, red) vs *R23E10-GAL4>UAS-mCherry RNAi* (black) and +; *UAS-RNAi* (gray) controls. For all groups, n ≥ 30 (Kruskall-Wallis with post-hoc Dunn's multiple comparison test). See **Table S3** for specific RNAi lines used. **Related to Figure 7**

A HMM fit to *iso31* D5-7 fly locomotor activity in the DAM5H system:

		Transition to:				Emission probability:	
		Deep sleep	Light sleep	Light wake	Full wake	Inactivity	Activity
Transition from:	State						
	Deep sleep	0.96	0.00	0.04	0.00	1.00	0.00
	Light sleep	0.07	0.72	0.21	0.00	1.00	0.00
	Light wake	0.00	0.43	0.24	0.32	0.01	0.99
Full wake	0.00	0.07	0.00	0.93	0.04	0.96	

B HMM fit to *iso31* D1 fly locomotor activity in the DAM5H system:

		Transition to:				Emission probability:	
		Deep sleep	Light sleep	Light wake	Full wake	Inactivity	Activity
Transition from:	State						
	Deep sleep	0.99	0.00	0.01	0.00	1.00	0.00
	Light sleep	0.31	0.51	0.18	0.00	1.00	0.00
	Light wake	0.00	0.28	0.18	0.54	0.00	1.00
Full wake	0.00	0.03	0.00	0.97	0.02	0.98	

C HMM fit to *CS* D5-7 fly locomotor activity in the DAM5H system:

		Transition to:				Emission probability:	
		Deep sleep	Light sleep	Light wake	Full wake	Inactivity	Activity
Transition from:	State						
	Deep sleep	0.98	0.00	0.02	0.00	1.00	0.00
	Light sleep	0.04	0.73	0.23	0.00	1.00	0.00
	Light wake	0.00	0.21	0.77	0.02	0.17	0.83
Full wake	0.00	0.01	0.00	0.99	0.04	0.96	

D HMM fit to *w1118* D5-7 fly locomotor activity in the DAM5H system:

		Transition to:				Emission probability:	
		Deep sleep	Light sleep	Light wake	Full wake	Inactivity	Activity
Transition from:	State						
	Deep sleep	0.99	0.00	0.01	0.00	1.00	0.00
	Light sleep	0.31	0.51	0.18	0.00	1.00	0.00
	Light wake	0.00	0.28	0.18	0.54	0.00	1.00
Full wake	0.00	0.03	0.00	0.97	0.02	0.98	

E HMM fit to *iso31* D5-7 fly locomotor activity from single-beam DAM system:

		Transition to:				Emission probability:	
		Deep sleep	Light sleep	Light wake	Full wake	Inactivity	Activity
Transition from:	State						
	Deep sleep	0.96	0.00	0.04	0.00	1.00	0.00
	Light sleep	0.07	0.72	0.21	0.00	1.00	0.00
	Light wake	0.00	0.43	0.24	0.32	0.01	0.99
Full wake	0.00	0.07	0.00	0.93	0.04	0.96	

F HMM fit to *elav-GAL4; + (attP40)* D5-7 fly activity from single-beam DAM system:

		Transition to:				Emission probability:	
		Deep sleep	Light sleep	Light wake	Full wake	Inactivity	Activity
Transition from:	State						
	Deep sleep	0.98	0.00	0.02	0.00	1.00	0.00
	Light sleep	0.08	0.67	0.25	0.00	1.00	0.00
	Light wake	0.00	0.17	0.80	0.03	0.29	0.71
Full wake	0.00	0.02	0.00	0.98	0.16	0.84	

G HMM fit to *R23E10-GAL4 > UAS-mCherry RNAi* D5-7 fly activity from DAM5H system:

		Transition to:				Emission probability:	
		Deep sleep	Light sleep	Light wake	Full wake	Inactivity	Activity
Transition from:	State						
	Deep sleep	0.98	0.00	0.02	0.00	1.00	0.00
	Light sleep	0.06	0.78	0.16	0.00	1.00	0.00
	Light wake	0.00	0.17	0.80	0.02	0.13	0.87
Full wake	0.00	0.01	0.00	0.99	0.03	0.97	

Table S1. All HMM parameters: Related to Figures 1-7. HMM parameters used in this paper, described as transition probabilities between hidden states and emission probabilities from each hidden state to observed states for HMMs trained on locomotor data from A) mature *iso31* flies (n = 87 flies), B) juvenile *iso31* flies (n = 82 flies), C) mature *Canton-S* flies (n = 95 flies), and D) mature *w1118* flies (n = 96 flies) collected using the DAM5H multibeam system. HMMs trained on locomotor data from E) mature *iso31* flies (n = 90 flies) and F) mature *elav-GAL4*;+ (*attP40*) flies (n = 46 flies) collected using the single beam DAM system. G) HMM trained on locomotor data from mature *R23E10-GAL4 > UAS-mCherry RNAi* flies (n = 31 flies) collected using the multibeam DAM system. A total of 1439 transitions per fly per 24 hours were used to train each model.

A

Gene set name	# genes in gene set	Enrichment score	Normalized enrichment score	Nominal p-value	FDR q-val
RIBONUCLEOPROTEIN COMPLEX	25	0.8334325	3.3576221	0	0
STRUCTURAL CONSTITUENT OF RIBOSOME	23	0.7740875	3.0646384	0	0
RIBOSOME	23	0.7740875	3.0391607	0	0
CYTOSOLIC PART	23	0.7740875	3.0359354	0	0
STRUCTURAL MOLECULE ACTIVITY	23	0.7740875	3.0340197	0	0
RIBOSOMAL SUBUNIT	23	0.7740875	3.0132124	0	0
CYTOSOLIC RIBOSOME	23	0.7740875	3.0076745	0	0
MITOTIC CELL CYCLE PROCESS	15	0.5640415	2.0024745	0.00466201	0.00371607
MICROTUBULE CYTOSKELETON ORGANIZATION	15	0.5558247	1.9938301	0.00943396	0.00354415
MICROTUBULE BASED PROCESS	15	0.5558247	1.9627372	0.00485437	0.00352023
CYTOSKELETON ORGANIZATION	15	0.5558247	1.9592851	0	0.00320021
MITOTIC CELL CYCLE	16	0.5014893	1.7472951	0.01678657	0.01589365
PROTEIN COMPLEX SUBUNIT ORGANIZATION	15	0.46264157	1.6513298	0.02849741	0.02640818

B

Gene	Neurodevelopment	Synaptic transmission	Ion homeostasis
Cbp53E	Blue	Gray	Gray
ringer	Blue	Gray	Gray
CG45263	Blue	Gray	Gray
miple1	Blue	Gray	Gray
14-3-3zeta	Blue	Blue	Gray
Syx1A	Blue	Blue	Gray
Cam	Blue	Blue	Gray
nSyb	Blue	Blue	Gray
twz	Gray	Gray	Blue
Vha14-1	Gray	Gray	Blue
Vha36-1	Gray	Gray	Blue
VhaM8.9	Gray	Gray	Blue
Vha13	Gray	Gray	Blue
Vha16-1	Gray	Gray	Blue
Vha55	Gray	Gray	Blue
porin	Gray	Gray	Blue
ATPsynC	Gray	Gray	Blue
jdp	Gray	Gray	Gray
CG7582	Gray	Gray	Gray
CG8974	Gray	Gray	Gray
TM4SF	Gray	Gray	Gray
CG32700	Gray	Gray	Gray
CG31808	Gray	Gray	Gray
CG3662	Gray	Gray	Gray
RNASEK	Gray	Gray	Gray
Rpl15	Gray	Gray	Gray
Drat	Gray	Gray	Gray

Table S2. GSEA and related GO terms for genes with differential expression in

juvenile vs mature flies: Related to Figure 7. A) GSEA results for DEGs with

increased expression in mature compared to juvenile dFB cells. B) Associated GO

terms for DEGs with increased expression in juvenile fly dFB cells. Blue boxes indicate

a given gene is associated with the listed GO term, while gray indicates the gene is not

associated with a GO term.

Gene	TRiP hairpin	BDSC #
14-3-3zeta	JF02962	28327
	HM04002	31498
	GL01310	41878
ATPsynC	GL00390	35464
CG32700	HMC04908	57719
CG3662	HMC05026	60033
CG7582	HMJ21718	53002
jdp	HMC06433	67329
porin	JF03251	29572
	HMS05687	67873
ringer	HMS01740	38287
twz	JF01867	25846
	HMC04701	57397
Vha13	CG6213	38233
Vha16-1	HMS02171	40923
Vha55	CG17369	40884

Table S3, all RNAi lines used for screen: Related to Figure 7. Screened RNAi lines for DEGs with higher expression in juvenile dFB cells.